Precambrian Research 362 (2021) 106301

Contents lists available at ScienceDirect

Precambrian Research

journal homepage: www.elsevier.com/locate/precamres

Tracing the Sveconorwegian orogen into the Caledonides of West Norway: Geochronological and isotopic studies on magmatism and migmatization

Cheng-Cheng Wang [a,*], Johannes D. Wiest [a,b], Joachim Jacobs [a], Bernard Bingen [c], Martin J. Whitehouse [d], Marlina A. Elburg [e], Thea S. Sørstrand [a], Lise Mikkelsen [a], Åse Hestnes [a]

[a] Department of Earth Science, University of Bergen, PB7803, N-5020 Bergen, Norway
[b] Geozentrum Nordbayern, Friedrich-Alexander-Universität Erlangen-Nürnberg, 91054 Erlangen, Germany
[c] Geological Survey of Norway, 7491 Trondheim, Norway
[d] Department of Geosciences, Swedish Museum of Natural History, Stockholm, Sweden
[e] Department of Geology, University of Johannesburg, Auckland Park 2006, Johannesburg, South Africa

ARTICLE INFO

Keywords:
Mesoproterozoic
Baltica
Zircon U–Pb geochronology
Hf–O isotopes
Collisional orogen
Rodinia

ABSTRACT

The Sveconorwegian orogen represents a branch of Grenville-age (~1250–950 Ma) orogenic belts that formed during the construction of the supercontinent Rodinia. This study traces the Sveconorwegian records from its type-area in the Baltic Shield of South Norway into basement windows underneath Caledonian nappes, by combining zircon U–Pb geochronology and Hf–O isotopes. Samples along a N-S trending transect reveal multiple magmatic episodes during Gothian (ca. 1650 Ma), Telemarkian (ca. 1500 Ma) and Sveconorwegian (1050–1020 Ma vs. 980–930 Ma) orogenesis as well as Sveconorwegian migmatization (1050–950 Ma). Newly documented 1050–1020 Ma magmatism and migmatization extend the Sirdal Magmatic Belt to a 300 km-long, NNW-SSE trending crustal domain, with the northern boundary corresponding to the gradual transition from Telemarkian to Gothian crust. These Precambrian crustal heterogeneities largely controlled the development of Caledonian shear zones. The ca. 1050–1040 Ma granitic and mafic magmas show similar isotopic signatures with slightly negative or positive εHf(t) and moderate $\delta^{18}O$ values (6–7‰), which indicates that crustal reworking was more dominant than juvenile inputs during their genesis. The generation of leucosomes and leucogranites at ca. 1030–1020 Ma, which have a more evolved Hf isotopic composition, probably reflects an even higher degree of remelting of older crust. The Hf–O isotopic patterns show that Sveconorwegian magmas differ from typical arc magmas by lower involvement of sedimentary components and juvenile material. This makes the 1050–930 Ma magmatism incompatible with a long-term subduction setting. The ca. 1650–1500 Ma samples, in contrast, generally have juvenile Hf isotopic compositions associated with varying $\delta^{18}O$ values of 4.5–9‰, consistent with subduction-accretion processes involving significant sedimentary recycling. This accretionary margin was most likely transformed into the Sveconorwegian orogen through collisional interactions of Baltica, Laurentia and Amazonia in the context of Rodinia amalgamation.

1. Introduction

Baltica records a long-lived orogenic history associated with the formation of the supercontinent Columbia/Nuna and its breakup and reassembly into Rodinia. Svetlana Bogdanova, honored in this special volume, made a career-long effort to correlate the geology across continents to give substance to models of assembly and breakup of these supercontinents (Gorbatschev and Bogdanova, 1993; Bogdanova et al., 2008, 2015). The southwestern margin of Baltica has been interpreted as an active continental margin that probably witnessed a continuous process of crustal accretion and growth during the Paleo- and Mesoproterozoic (Gorbatschev and Bogdanova, 1993; Åhäll and Larson, 2000; Andersen et al., 2002; Roberts and, 2015), and was subsequently overprinted by the Grenville-age Sveconorwegian orogeny during Rodinia assembly (Fig. 1a, Bogdanova et al., 2008). The Sveconorwegian orogenic evolution remains a hot topic of debate, although much has been published on the many very varied aspects of geology, geophysics and geochemistry in recent years (e.g. Bingen and Viola,

* Corresponding author.
E-mail address: Cheng-Cheng.Wang@uib.no (C.-C. Wang).

https://doi.org/10.1016/j.precamres.2021.106301
Received 4 January 2021; Received in revised form 26 May 2021; Accepted 2 June 2021
Available online 9 July 2021

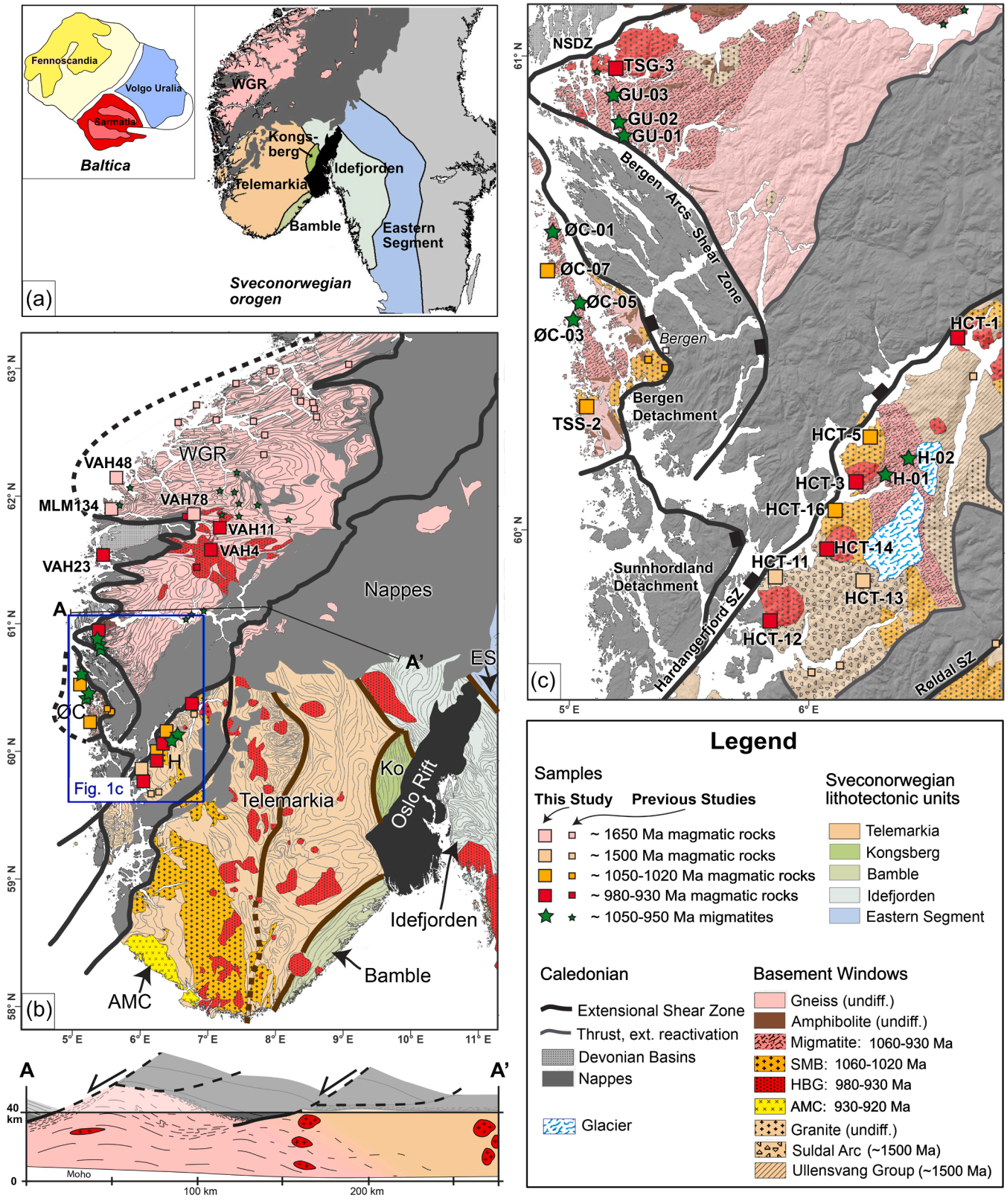

Fig. 1. (a) Tectonic sketch map of Baltica (after Bogdanova et al., 2008) and the Sveconorwegian orogen; (b) Geologic overview map of South Norway, showing the distribution of Sveconorwegian crust, its relation to the Caledonian province (nappes) to the north and location of the study area with samples localities in the WGR; schematic cross section (A-A', modified from Milnes et al., 1997) showing the structural relationship between the undeformed Baltic Shield and variably deformed crust (schematically represented by the shape of granites) exposed in the Caledonian basement windows; (c) Newly compiled geologic map of the study area, with igneous and migmatite samples from the Øygarden Complex and the Hardangerfjord area. The interpreted distribution of Sveconorwegian crustal ages is based on new and previously published U–Pb zircon geochronology. Abbreviations: AMC, Anorthosite–Mangerite–Charnockite suite; ES, Eastern Segment; H, Hardangerfjord area; HBG, hornblende-biotite granite; Ko, Kongsberg unit; NSDZ, Nordfjord-Sogn Detachment Zone; ØC, Øygarden Complex; SMB, Sirdal Magmatic Belt; SZ, shear zone; WGR, Western Gneiss Region.

2018; Slagstad et al., 2018a,b, 2020; Stephens, 2020; Bingen et al., 2021). In archetypal reconstructions of Rodinia, Laurentia is located in the centre of Rodinia, with Baltica to the east and Amazonia to the south and the Sveconorwegian orogen facing the northern margin of Amazonia (present coordinates) (Hoffman, 1991; Torsvik et al., 1996; Dalziel, 1997; Li et al., 2008; Cawood and Pisarevsky, 2017; Merdith et al., 2017). The Kalahari craton is regarded as another core constituent of the Rodinia landmass on the western side of the supercontinent, as supported by both paleomagnetic and geological studies (Dalziel et al., 2000; Jacobs et al., 2008; Swanson-Hysell et al., 2015, 2019).

During and after Rodinia breakup, the margins of Laurentia, Baltica and Amazonia were affected by two Wilson cycles from the late Neoproterozoic to the Mesozoic. These cycles involved the opening and closing of the Iapetus Ocean, formation of the Caledonian and Appalachian orogens, and opening of the Atlantic Ocean (Torsvik et al., 1996; Bingen et al., 1998; Cawood et al., 2001; Cocks and Torsvik, 2005). Portions of the margins of Laurentia, Baltica and Amazonia, characterized by Mesoproterozoic magmatism and metamorphism, are now located in basement windows (inliers) and in thrust nappes in the Caledonides of Scandinavia, the British Isles and Greenland, and the Appalachian Mountains of Canada and the USA (McLelland et al., 2010; Roffeis and Corfu, 2014). In West Norway, the Baltican basement is largely exposed underneath vast thrust sheets (Fig. 1b), and the intersection between the Caledonian and Sveconorwegian orogens makes it a challenging but interesting issue to clarify the northward extension of the Sveconorwegian Province (e.g. Lorenz et al., 2012; Gee et al., 2015). Investigating these basement windows is crucial to understand the composition and evolution of the continental crust, determine the distribution of the orogenic domains, and reconstruct the Grenville-age orogeny during Rodinia assembly.

In this paper, we address the geology, geochronology and isotope geochemistry of four parts of the Baltican basement in West Norway that represent variable states of Caledonian reworking (Fig. 1). Corresponding to increasing strain from southeast to northwest, they are the Hardangerfjord area (Fossen and Hurich, 2005), the Øygarden Complex (Wiest et al., 2020a) and the southern and central parts of the Western Gneiss Region (Gulen dome (Wiest et al., 2019) and Nordfjord area (Labrousse et al., 2004)). We report zircon U–Pb, Lu–Hf and O isotopic data on zircons from magmatic rocks and leucosomes from migmatites. By constraining the magmatic and metamorphic events, we explore the relation between the basement windows and the type-area of the Sveconorwegian orogen in southwest Norway, and thereby trace the Sveconorwegian orogeny northwards. Furthermore, the review and comparison of Mesoproterozoic orogenesis along the margins of Baltica, Laurentia and Kalahari allow for a better understanding of the tectonic evolution of Grenville-age orogenic belts in the core of Rodinia.

2. Geological setting

2.1. The Sveconorwegian orogen

The Sveconorwegian orogen (ca. 1150–900 Ma) is a ca. 550 km wide orogenic zone covering south Norway and southwest Sweden (Fig. 1a). It can be divided into five main lithotectonic units/terranes separated by N-S-trending crustal-scale shear zones. From the Sveconorwegian front in the east towards the west these are: the Eastern Segment, the Idefjorden, Kongsberg, Bamble and Telemarkia lithotectonic units (Bingen et al., 2008a, 2021). The Sveconorwegian orogen was built on the Paleo-Mesoproterozoic continental lithosphere. In general, the formation of the first lithosphere in these five units occurred progressively later towards the west: in the Eastern Segment as part of the 1710–1660 Ma Transcandinavian Igneous Belt, at 1660–1520 Ma during the Gothian orogeny in the Idefjorden, Bamble and Kongsberg units, and at 1520–1480 Ma during the Telemarkian orogeny in the Telemarkia unit (Bingen et al., 2005; Roberts and Slagstad, 2015). After lithosphere formation, the Eastern Segment was affected by the 1.47–1.38 Ga Hallandian accretionary orogeny, which has been scarcely reported in the remaining of the Sveconorwegian orogen to the west of the Eastern Segment (Ulmius et al., 2015).

The five lithotectonic units are characterized by distinct Sveconorwegian magmatic and metamorphic histories. The Eastern Segment appears to be distinct from the other four units by lacking >1000 Ma Sveconorwegian events. It is characterized by ca. 990 Ma eclogite-facies metamorphism with estimated peak P-T conditions at 860–900 °C/1.65–1.8 GPa (Möller et al., 2015; Tual et al., 2017). This metamorphism was interpreted to reflect underthrusting of the Eastern Segment beneath the lithotectonic units to the west (Möller and Andersson, 2018). The Idefjorden unit contains evidence for 1050–1020 Ma granulite-facies metamorphism and several pulses of magmatism between 1040 and 910 Ma (Bingen et al., 2008b; Söderlund et al., 2008; Bergström et al., 2020). In the Kongsberg and Bamble units, high-grade metamorphism is older at 1150–1120 Ma (Cosca et al., 1998; Bingen et al., 2008b; Engvik et al., 2016; Bingen and Viola, 2018). The Telemarkia unit features 1050–930 Ma granitic magmatism, 930–920 Ma anorthosite–mangerite–charnockite magmatism and associated high-grade metamorphism (more details below). Distinct Sveconorwegian magmatic and metamorphic records in the five lithotectonic units reflect a complex orogenic history. Therefore, there are distinct views in the literature on the formation and evolution of the Sveconorwegian orogen, and contrasting tectonic models have been proposed (see review in Bingen et al., 2021 and references therein). In general, the debate centers on whether the Sveconorwegian orogen represents an accretionary orogen with long-term subduction, or a continental collision orogen that can be regarded as an extension of the Grenville Orogen in Laurentia (e.g. Bingen and Viola, 2018; Möller and Andersson, 2018; Slagstad et al., 2020; Bingen et al., 2021).

2.2. The Telemarkia unit

The Telemarkia crust mainly formed during three episodes of magmatic events, at 1520–1480 Ma, 1280–1140 Ma and 1060–930 Ma (Andersen et al., 2001, 2007, Bingen et al., 2005, 2008c; Pedersen et al., 2009; Roberts et al., 2013; Roberts and Slagstad, 2015). The 1520–1480 Ma event (Telemarkian) is interpreted as a supra-subduction accretionary event, with voluminous volcanic arc lithologies towards the west (the Suldal volcanic arc; Roberts et al., 2013) and back-arc rift lithologies towards the east (the Rjukan rift). The 1280–1140 Ma rocks are mainly bimodal plutonic and volcanic suites as well as associated sedimentary rocks, which formed in the 1280–1240 Ma, 1230–1200 Ma and 1180–1140 Ma time intervals. The 1060–930 Ma Sveconorwegian *syn*-orogenic magmatic rocks include three main plutonic suites, the 1060–1020 Ma Sirdal Magmatic Belt (SMB), the 980–930 Ma hornblende-biotite granite suite (HBG) and the 930–920 Ma Rogaland anorthosite–mangerite–charnockite suite (Vander Auwera et al., 2011; Granseth et al., 2020) (Fig. 1b). The SMB is a >150 km long, NNW-SSE trending batholith exposed from the southern tip of Norway and disappearing northwards under Caledonian nappes (Slagstad et al., 2013). It is mainly composed of porphyritic amphibole-biotite and biotite granitoids, associated with leucogranite and garnet granite (Coint et al., 2015). These rocks have a high-K calc-alkaline geochemical signature (Slagstad et al., 2013; Bingen et al., 2015) that may reflect inheritance from the source rocks, i.e. the 1520–1480 Ma calc-alkaline rocks of the Suldal volcanic arc (Coint et al., 2015). The 980–930 Ma HBG suite occurs as discrete granitoid plutons with a ferroan 'A-type' geochemical signature, cropping out in the area defined by the SMB and east of it (Bogaerts et al., 2003; Vander Auwera et al., 2011; Granseth et al., 2020). The 930–920 Ma Rogaland anorthosite–mangerite–charnockite suite, exposed in the westernmost part of the orogen, is a Proterozoic massif-type anorthosite plutonic complex, which is anhydrous with an alkalic ferroan geochemical signature (Fig. 1b; Ashwal, 1993; Schärer et al., 1996; Vander Auwera et al., 2011).

The metamorphic grade increases southwestwards in the Telemarkia

unit towards the Rogaland anorthosite–mangerite–charnockite plutonic complex. Three isograds are mapped, the orthopyroxene-in, osumilite-in and pigeonite-in isograds (Tobi et al., 1985). Metamorphic zircon and monazite define a wide range of U–Pb apparent ages ranging from ca. 1050 to 920 Ma (Möller et al., 2002; Tomkins et al., 2005; Bingen et al., 2008a; Drüppel et al., 2013; Blereau et al., 2017; Laurent et al., 2018a,b; Slagstad et al., 2018a), suggesting that this region underwent long-lived high-grade metamorphism. In more detail, two distinct metamorphic events can be recognized, both reaching ultra-high temperature (>900 °C) conditions. The first event is interpreted as part of a long-lived regional metamorphic event, peaking at ca. 0.6 GPa/920 °C and dated between ca. 1045 and 990 Ma, while the second event, peaking at ca. 4.5 GPa/900 °C, was closely related to the intrusion of the anorthosite–mangerite–charnockite complex at ca. 930 Ma (Drüppel et al., 2013; Blereau et al., 2017; Laurent et al., 2018a, 2018b).

2.3. The Caledonian orogen

Break-up of Rodinia and the opening of the Iapetus Ocean in the Neoproterozoic formed a segmented passive margin of Baltica (e.g. Jakob et al., 2019). Subsequent closure of the Iapetus in the Paleozoic resulted in the Caledonian orogeny, which culminated with the collision between Laurentia, Avalonia and Baltica in the Silurian–Devonian (Scandian orogeny) (Corfu et al., 2014a). Various parts of the Laurentian margin, the Iapetus oceanic realm and the distal domains of the Baltican margin were thrust onto Baltica, while the western margin of Baltica was subducted below Laurentia down to mantle depths (Brueckner, 2018). Continent-continent collision was swiftly followed by a change from plate convergence to divergence (Fossen, 1992; Rey et al., 1997). Early Devonian transtensional collapse formed an orogen-wide network of extensional detachments and supra-detachment basins (Fossen, 2010) and resulted in the diachronous exhumation of the former orogenic infrastructure in metamorphic core complexes of variable size (Wiest et al., 2021). Later extensional episodes, related to North Sea rifting, took place from the Permian throughout the Mesozoic, reactivating the previously formed crustal template in a brittle fashion (Fossen et al., 2016; Ksienzyk et al., 2016; Peron-Pinvidic and Osmundsen, 2020; Wiest et al., 2020b).

2.4. Geology of the studied areas

2.4.1. Western Gneiss Region (WGR)

The WGR represents a giant (>30,000 km^2) basement window underneath the Caledonian nappes, exposing the Proterozoic Baltican margin that was subducted to (ultra)high-pressure metamorphism and variably deformed (Milnes et al., 1997; Wain, 1997; Hacker et al., 2010) (Fig. 1b). The WGR mainly consists of migmatitic orthogneisses with dioritic to granitic compositions. The protoliths formed mostly during the Gothian orogeny around 1650 Ma (Bingen et al., 2005) and were intruded by mafic dykes at 1470–1450 and 1260–1250 Ma (Austrheim et al., 2003; Krogh et al., 2011; Beckman et al., 2014). Except for the north-easternmost part of the WGR, there is abundant evidence for Sveconorwegian reworking, including widespread migmatization, granitic magmatism and granulite-facies metamorphism (Tucker et al., 1990; Skår and Pedersen, 2003; Røhr et al., 2004; Glodny et al., 2008; Gordon et al., 2013; Røhr et al., 2013; Kylander-Clark and Hacker, 2014). Ages of Sveconorwegian granites and migmatites in the WGR fall exclusively in the range between ca. 980 and 940 Ma (e.g. Skår and Pedersen, 2003; Gordon et al., 2013; Røhr et al., 2013; Kylander-Clark and Hacker, 2014). In contrast to the Sveconorwegian orogen in southwest Norway, 1060–1020 Ma intrusives have not been reported.

This study addresses the Nordfjord and Gulen areas, which constitute a transect from ultra high-pressure to high-pressure conditions of Caledonian reworking in the Baltican basement. The Nordfjord domain represents the southernmost occurrence of ultra high-pressure minerals and furthermore records migmatization and intense shearing during extensional collapse (Labrousse et al., 2002, 2004; Kylander-Clark and Hacker, 2014). The Gulen area defines a metamorphic core complex in the southernmost WGR, the Gulen dome, which exhumed strongly deformed, eclogite-bearing crust during Devonian collapse (in the footwall of the extensional Bergen Arcs Shear Zone and the Nordfjord-Sogn detachment) (Wiest et al., 2019). Like other parts of the WGR, eclogites are hosted in migmatites, but based on field observations, Wiest et al. (2019) inferred that Caledonian deformation involved exclusively solid-state shearing and, hence, migmatization must be older. Granulite-facies rocks along the rim of a weakly deformed granite-diorite pluton revealed Tonian U–Pb zircon (ca. 980 Ma) and monazite (ca. 950 Ma) ages (Røhr et al., 2004), while the Caledonian shear zones are associated with Ar-Ar mica ages mostly in the range from 405 to 393 Ma (Wiest et al., 2021).

2.4.2. Øygarden Complex

The Øygarden Complex is the southernmost Devonian metamorphic core complex along the west coast of South Norway (Wiest et al., 2020a). It is separated from the neighbouring Gulen dome by the Bergen Arcs Shear Zone (Fig. 1c) (Wennberg et al., 1998) and in contrast to the former, no eclogites have been documented in this region. The eastern (structurally higher) part of the Øygarden Complex consists of a Sveconorwegian magmatic complex, comprising ca. 1040 Ma granites and gabbros as well as 1020 Ma leucogranites, intruding Telemarkian (1500 Ma) granitic basement (Wiest et al., 2018). The western (structurally lower) part of the Øygarden Complex consists mostly of migmatites with granitic to dioritic compositions and associated leucogranites. The migmatites at the deepest levels of the dome are evidently Caledonian and crystallized at ca. 405 Ma, but preserve also Sveconorwegian ages (Wiest et al., 2021). The entire complex was strongly sheared (Wiest et al., 2020a) during core-complex exhumation between 405 and 398 Ma (Wiest et al., 2021).

2.4.3. Hardangerfjord area

The Hardangerfjord runs along a major Devonian extensional shear zone, the Hardangerfjord shear zone, that juxtaposes Caledonian nappes in the NW, above a Proterozoic basement little affected by Caledonian reworking in the SE (Fig. 1c) (Fossen and Hurich, 2005). As such, the Hardangerfjord shear zone represents the southernmost limit of thick-skinned deformation during Caledonian extensional collapse (Fossen et al., 2014). Towards the SE, this Proterozoic basement is largely covered by Caledonian nappes, called the Hardangervidda-Ryfylke nappe complex, in such a way that the continuity of outcrop between the Proterozoic rocks in the Hardangerfjord area and the Telemarkia lithotectonic unit of the Sveconorwegian orogen is only locally observable (Roffeis et al., 2013). On geological maps, the Proterozoic basement in the Hardangerfjord area is directly correlated with the Telemarkia lithotectonic unit further south and considered as integral part of it (Bingen et al., 2005; Sigmond, 1998). However, actual data to support this correlation are scant.

The Proterozoic basement in the Hardangerfjord area consists of large NNW-SSE-trending granite plutons, which intrude tracts of tonalitic to gabbroic rocks and supracrustal sequences (Torske, 1982). Metavolcanic rocks within the latter have a Telemarkian (1500 Ma) age (Bingen et al., 2005) similar to gabbros and granites in the Suldal volcanic arc further south (Roberts et al., 2013). Caledonian extensional deformation was highly localized into weak lithologies in the nappes and a narrow shear zone in the basement, leaving most of the Precambrian lithologies in this area virtually undeformed.

3. Methods

This study involves twenty-five newly collected igneous and migmatite samples from the Hardangerfjord area, the Øygarden Complex and the WGR as well as six igneous samples dated by Wiest et al. (2018). Selected zircon grains were mounted in epoxy and polished. Prior to

U–Pb analyses, images were collected with optical microscopy (reflected and transmitted light) and with a cathodoluminescence (CL) detector in a scanning electron microscope, to reveal the internal textures of zircon and select analytical spots. U–Pb, Lu–Hf and O isotopic analyses were performed as much as possible on the same spot or from the same growth zone. Detailed analytical methods are described in Supplementary File A.

Zircon U–Pb dating was carried out using a CAMECA IMS-1280 instrument at the NordSIM laboratory, Swedish Museum of Natural history, Stockholm. Weighted mean ages and concordia ages are calculated with the program Isoplot (Version 4.15). All errors are reported at the 2σ-level. Oxygen isotope ratios of zircon were measured with the same instrument with a Cs source. Prior to O analysis, the U–Pb analysis pits were removed by polishing. The values of average $\delta^{18}O$ values are reported as mean ± standard deviation (S.D.).

Lu–Hf isotopes were measured at the University of Johannesburg, using an ASI Resonetics 193 nm Excimer laser ablation system coupled to a Nu Plasma II multi-collector ICPMS. Initial epsilon Hf values (εHf(t)) were calculated using a decay constant of 1.867×10^{-11} (Scherer et al., 2001; Söderlund et al., 2004), and CHUR models of Bouvier et al. (2008) ($^{176}Lu/^{177}Hf$ and $^{176}Hf/^{177}Hf$ of 0.0336 and 0.282785, respectively). The calculation of model ages is based on the depleted mantle model of Griffin et al. (2000) with present-day $^{176}Hf/^{177}Hf = 0.28325$ and $^{176}Lu/^{177}Hf = 0.0384$. Initial $^{176}Hf/^{177}Hf$ and epsilon Hf values for analyzed zircons from magmatic rocks were calculated using the respective interpreted crystallization age of each sample. For anatectic zircons from leucosomes in migmatites, the concordia age interpreted as the crystallization age of the melts were used, although some samples may record multiple periods of partial melting and migmatization. The values of average εHf(t) and $^{176}Hf/^{177}Hf_{(i)}$ for each sample are reported

Table 1
Summary of geochronology and Hf-O isotopic results of magmatic samples in this study.

Sample	Longitude (E)	Latitude (N)	Rock types	Main mineral composition	Igneous age (Ma)			εHf (t)	$\delta^{18}O$ (‰)
					concordia age	**weighted mean $^{207}Pb/^{206}Pb$ age**	**weighted mean $^{206}Pb/^{238}U$ age**		
Hardangerfjord area									
HCT-11	5.83297	59.93082	Tonalitic gneiss	Qz + Pl + Amp + Bt + Grt + Chl	1528 ± 7	1516 ± 6	1541 ± 8	6.9 ± 0.7	4.5 ± 0.2
HCT-13	6.20977	59.93102	Tonalitic gneiss	Qz + Pl + Amp + Bt	1516 ± 6	1509 ± 8	1529 ± 10	4.8 ± 0.8	4.6 ± 0.2
HCT-16	6.07065	60.07829	Granite	Kfs + Qz + Pl + Bt + Ms + Spn	1042 ± 9	1029 ± 12	1051 ± 8	0.4 ± 0.5	6.4 ± 0.3
HCT-5	6.20556	60.23750	Augen gneiss	Pl + Qz + Kfs + Amp + Bt + Spn	1045 ± 5	1035 ± 8	1048 ± 5	0.7 ± 0.7	6.4 ± 0.2
HCT-3	6.14859	60.13702	Foliated granite	Qz + Kfs + Pl + Bt + Ms + Spn + Mnz	978 ± 4	964 ± 8	980 ± 4	–2.0 ± 0.5	5.6 ± 0.3
HCT-14	6.04722	59.99917	Granite	Qz + Pl (secondary alteration) + Kfs + Bt + Spn + Ep	944 ± 5	914 ± 15	948 ± 5	–0.8 ± 0.6	6.4 ± 0.3
HCT-12	5.82155	59.83664	Foliated granite	Qz + Kfs + Pl (secondary alteration) + Bt + Ms	944 ± 6	923 ± 13	948 ± 6	2.6 ± 0.6	5.9 ± 0.2
HCT-1	6.55885	60.45515	Granite	Qz + Pl (secondary alteration) + Kfs + Bt + Ms + Grt + Spn	938 ± 11	937 ± 32	938 ± 12	–3.7 ± 0.7	6.7 ± 0.4
Øygarden Complex									
LYD83-1[a]	5.25992	60.38736	Mylonitic granitic gneiss	Qz + Pl + Bt + Kfs	1506 ± 5	1501 ± 4	1515 ± 8	3.9 ± 0.9	8.5 ± 0.3
LYD44-1[a]	5.23914	60.37553	Metagabbro	Amp + Opx + Pl	1041 ± 3	1035 ± 8	1044 ± 5	1.8 ± 0.6	6.3 ± 0.2
LYD197-1[a]	5.24186	60.37358	Hornblende biotite granite gneiss	Kfs + Qz + Amp + Pl + Bt	1041 ± 3	1039 ± 7	1042 ± 3	1.2 ± 0.9	6.3 ± 0.2
LYD35-1[a]	5.23156	60.37714	Amphibolite	Amp + Pl	1040 ± 11	1026 ± 9	1037 ± 17	–0.2 ± 1.3	6.3 ± 0.3
TSS-2	4.99556	60.26667	Augen gneiss	Qz + Kfs + Pl + Bt + Ms + Ap	1036 ± 5	1036 ± 7	1035 ± 11	0.5 ± 1.0	6.4 ± 0.3
LYD169-1[a]	5.24958	60.36792	Mylonitic granitic gneiss	Qz + Kfs + Pl + Bt	1027 ± 4	1020 ± 4	1032 ± 5	–2.6 ± 0.8	6.5 ± 0.3
LYD163-1[a]	5.25992	60.38736	Gneissic leucogranite	Kfs + Pl + Qz + Ms + Bt	1022 ± 11	1022 ± 13	1031 ± 21	–2.4 ± 1.0	6.2 ± 0.7
Western Gneiss Region									
VAH78	6.49285	61.93872	Augen gneiss	Qz + Kfs + Pl + Bt + Ms + Ep	1653 ± 8	1648 ± 7	1671 ± 18	2.5 ± 0.7	9.1 ± 1.0
VAH48	5.18452	62.19870	Augen gneiss	Qz + Kfs + Pl + Bt + Ms + Ep	1651 ± 7	1649 ± 11	1656 ± 12	3.1 ± 0.7	8.4 ± 0.3
MLM134	5.13059	61.94703	Augen gneiss	Qz + Kfs + Pl + Bt + Ms + Ep	1621 ± 8	1624 ± 14	1610 ± 16	2.3 ± 0.8	8.9 ± 0.5
TSG-3	5.03647	60.98648	Foliated granite	Qz + Kfs + Pl + Bt + Spn + Mnz	966 ± 4	954 ± 9	969 ± 5	–2.5 ± 0.5	5.8 ± 0.2
VAH11	6.96253	61.84878	Foliated granite	Qz + Kfs + Pl + Bt + Ap	961 ± 8	939 ± 13	965 ± 8	–5.1 ± 0.6	6.8 ± 0.3
VAH4	6.82158	61.66319	Foliated granite	Qz + Kfs + Pl + Bt + Ap + Ep	958 ± 7	939 ± 15	962 ± 7	–5.3 ± 1.0	6.8 ± 0.2
VAH23	5.04299	61.58910	Foliated granite	Qz + Kfs + Pl + Bt + Ap	944 ± 7	917 ± 14	950 ± 9	–3.1 ± 0.7	6.4 ± 0.4

Samples with superscript 'a' were dated by Wiest et al. (2018). The concordia age is preferred to represent the crystallization age and be used for Hf isotopic calculation. Mineral abbreviations after Whitney and Evans, 2010.

as mean ± S.D.

4. Results, (meta)igneous rocks

Key information on the samples, including the lithologies, coordinates, U–Pb, Lu–Hf and O isotopic data, is summarized in Table 1.

4.1. Hardangerfjord area

4.1.1. Telemarkian (ca. 1520 Ma) tonalitic gneisses

Samples HCT-11 and HCT-13 are two grey tonalitic gneisses collected some 15 km apart. The outcrop of HCT-13 is weakly foliated and interlayered with amphibolite (Fig. 2a, b). Zircon crystals from these two samples exhibit broad CL-bright domains with oscillatory or banded zoning frequently surrounded by CL-dark rims, tips or prisms. In sample HCT-11, 16 analyses mostly on CL-bright, zoned domains give a concordia age at 1528 ± 7 Ma (MSWD = 1.6) (Fig. 2a). In sample HCT-13, 20 analyses were conducted on zoned domains, and 11 of them define a concordia age at 1516 ± 6 Ma (MSWD = 1.5) (Fig. 2b). These ages represent the crystallization age of the tonalite protolith.

Their Hf isotopic compositions are rather juvenile with mean εHf(t) values of + 6.9 ± 0.7 and + 4.8 ± 0.8 for HCT-11 and HCT-13 respectively; $\delta^{18}O$ values are in the range of or slightly lower than mantle value, and the average values are 4.5/4.6 ± 0.2‰.

4.1.2. Sveconorwegian (ca. 1050–930 Ma) granitoids

Sample HCT-16 is a weakly foliated porphyritic granite (Fig. 2c). Zircon crystals are usually subhedral, fractured and rich in inclusions. In CL images, most grains exhibit highly luminescent cores with oscillatory zoning surrounded by darker rims, tips or prisms. Some grains are entirely CL-dark with patchy and mosaic CL emission locally or along the margin, and have high contents of common lead, suggesting possible metamictization and alteration by hydrothermal fluids. Seventeen analyses were conducted on oscillatory zoned cores. One analysis, although slightly discordant (disc. 5.6%), gives a $^{207}Pb/^{206}Pb$ age at ca. 1480 Ma, indicating zircon inheritance. Eight concordant analyses on zoned domains define a concordia age at 1042 ± 9 Ma (MSWD = 1.9) (Fig. 2c), which is interpreted as the crystallization age of the granite. Eight analyses on rims are mostly slightly discordant ranging from 1050 to 460 Ma ($^{206}Pb/^{238}U$ ages), and reflect varying degrees of resetting of U–Th–Pb system. Two concordant analyses give an age at ca. 460 Ma, which may represent the time of metamorphic resetting. The Hf isotopic compositions defined by 8 concordant spots yield εHf(t) values of +0.4 ± 0.5. All analyses have similar O isotopic composition with an average $\delta^{18}O$ value of 6.4 ± 0.3‰.

Sample HCT-5 was collected from a heterogeneous outcrop consisting of a folded sequence of granitic to dioritic gneisses (Fig. 2d), intruded by granitic sheets, mafic dikes and pegmatite veins. It is a mesocratic granite with mafic clusters consisting of amphibole and biotite. Zircon grains are euhedral to subhedral, and most show oscillatory or banded zones occasionally surrounded by a dark rim (too narrow to be analyzed). Several zircons have homogeneous CL-dark cores; one analysis was slightly discordant at ca. 1270 Ma (disc. 3.9%), probably representing inheritance. Twenty analyses on zoned domains give a concordia age of 1045 ± 5 Ma (MSWD = 1.4) (Fig. 2d), representing the time of igneous crystallization. In this sample, 21 isotopic analyses on zoned domains give an average εHf(t) value of +0.7 ± 0.7, and an average $\delta^{18}O$ values of 6.4 ± 0.2‰.

HCT-3 is a foliated granite sample (Fig. 2e). Zircon grains are euhedral to subhedral, and commonly rich in mineral inclusions. In CL images, most crystals are dominated by oscillatory, banded or sector zones, and few ones have a thin and dark rim. Thirty-two analyses on zoned domains define a concordia age at 978 ± 4 Ma (MSWD = 1.03) (Fig. 2e), representing the time of igneous crystallization. In this sample, 16 analyses on zoned cores give an average εHf(t) value of −2.0 ± 0.5, and an average $\delta^{18}O$ value of 5.6 ± 0.3‰.

HCT-14 is a granite sample. Zircon grains are mostly euhedral, commonly rich in mineral inclusions, and are finely oscillatory in CL images. Twenty-seven analyses on zoned domains, except one that is excluded from the calculation because of a large uncertainty, define a concordia age at 944 ± 5 Ma (MSWD = 1.4) (Fig. 2f). This age represents the crystallization age of the sample. In addition, minor zircon grains are smaller and significantly darker in CL because of high U contents; one analysis yields a $^{206}Pb/^{238}U$ age at ca. 1025 Ma, which may represent zircon inheritance. Sixteen analyses on ca. 945 Ma zircon grains give an average εHf(t) value of −0.8 ± 0.6, and an average $\delta^{18}O$ values of 6.4 ± 0.3‰.

HCT-12 is a granite with abundant K-feldspar megacrysts up to 5 cm wide. Sampled at the rim of the circular pluton (Fig. 1c), a weak foliation is developed in the homogeneous exposure (Fig. 2g). In CL images, most grains show moderate to high luminosity with oscillatory or banded zones. Twenty-seven of 30 analyses define a concordia age at 944 ± 6 Ma (MSWD = 1.6) (Fig. 2g), recording the crystallization time of the granite. Seventeen analyses have an average εHf(t) value of +2.6 ± 0.6, and an average $\delta^{18}O$ value of 5.9 ± 0.2‰.

Sample HCT-1 is collected from an outcrop of grey isotropic equigranular granite, in the northern part of the Hardangerfjord area (Fig. 2h). Most zircon grains consist of a CL-bright core with oscillatory/banded zones surrounded by a CL-dark rim. In several grains, the rim domains or even the whole grain of several zircons show bright and patchy CL images, similar to the characteristics of metamict zircon altered by aqueous fluids. The dating results of 13 analyses on cores show two concordant age populations at 938 ± 11 Ma (n = 4, MSWD = 0.82) and 1052 ± 15 Ma (n = 3, MSWD = 1.7), respectively (Fig. 2h). The former is interpreted as the time of igneous crystallization, while the latter group together with two older analyses at 1.4–1.2 Ga probably represents zircon inheritance. Six analyses on rims are concordant or nearly concordant with $^{206}Pb/^{238}U$ ages ranging from ca. 890 to 450 Ma, and the youngest age at ca. 450 Ma is probably approaching the timing of formation of the rim. The Hf isotopic analyses on the four concordant ca. 938 Ma spots yield an average εHf(t) value of −3.7 ± 0.7. Oxygen isotopic analyses on both concordant and discordant spots have very a similar O isotopic composition with an average $\delta^{18}O$ value of 6.7 ± 0.4‰.

4.2. Øygarden Complex, Sveconorwegian (ca. 1050–1030 Ma) (meta) igneous rocks

TSS-2 is an augen gneiss sample (Fig. 2i). Zircon grains are euhedral to subhedral with roundish terminations, and most grains have a dominant oscillatory-zoned domain surrounded by thin, dark, structureless rims. Small, dark cores are observed in a few grains. Twenty-four analyses were performed on domains with oscillatory zones. Ten of them give a concordia age at 1036 ± 5 Ma (MSWD = 1.4) (Fig. 2i), which is interpreted as the crystallization time of the granite. Of the two analyses on rims, one has significantly low Th content and Th/U ratio (0.04) and is nearly concordant at ca. 960 Ma, probably representing the time of subsequent metamorphism. Nine analyses on zoned domains give an average εHf(t) value of +0.5 ± 1.0, and an average $\delta^{18}O$ value of 6.4 ± 0.3‰.

In addition, 6 samples from the mountain Lyderhorn, the Øygarden Complex, dated by Wiest et al. (2018), were also analyzed for Hf and O isotopic compositions, including one ca. 1500 Ma granitic gneiss and five Sveconorwegian 1040–1020 Ma mafic and granitic rocks. The oldest sample (LYD83-1, 1506 ± 5 Ma) is characterized by highly elevated $\delta^{18}O$ values of 8.5 ± 0.3‰ and positive εHf(t) values of +3.9 ± 0.9. The two mafic rocks (LYD35-1, 1040 ± 11 Ma; LYD44-1, 1041 ± 3 Ma) have near-chondritic εHf(t) values of –0.2 ± 1.3 and +1.8 ± 0.6 respectively, comparable to the value of coeval granitic rocks (LYD197-1, 1042 ± 3 Ma, εHf(t) = +1.2 ± 0.9). Two leucogranitic rocks (LYD163-1, 1022 ± 11 Ma; LYD169-1, 1027 ± 4 Ma) have more negative εHf(t) values of −2.4 ± 1.0 and −2.6 ± 0.8. The five Sveconorwegian samples have very

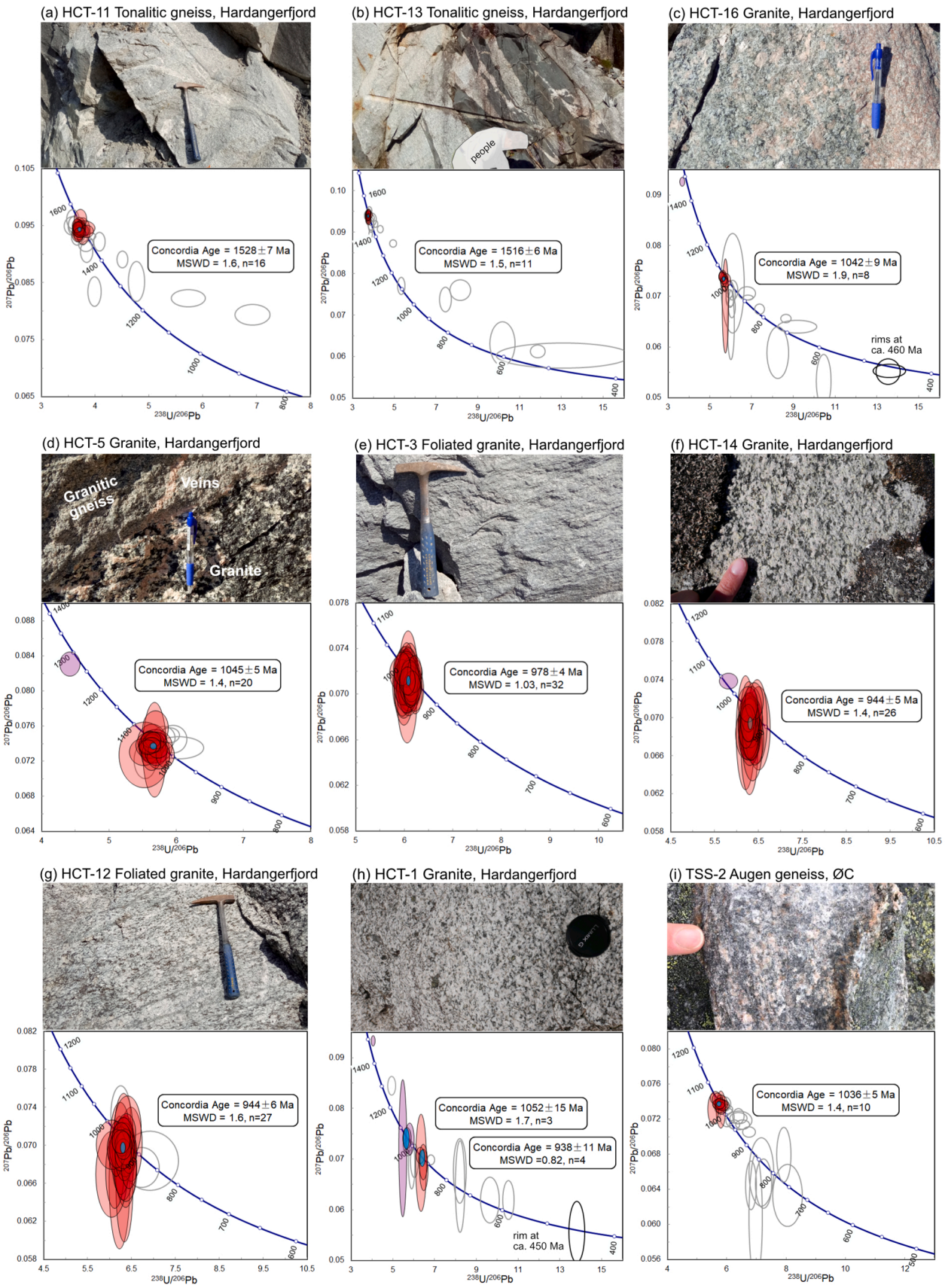

Fig. 2. Field outcrop photographs and zircon U–Pb Tera-Wasserburg diagrams of igneous samples from the Hardangerfjord and Øygarden Complex (ØC); red ellipses: igneous zircons used for calculation of concordia age (turquoise); purple: inherited zircons; grey: (reversely) discordant and Pb-loss analyses; black: Caledonian metamorphic rims. For details of each data-point see Table 1, Supplementary File B.

similar O isotopic compositions with average $\delta^{18}O$ values of 6.2–6.5‰.

4.3. Western Gneiss Region

4.3.1. Gothian (ca. 1650–1620 Ma) granitic gneisses

Samples VAH 78, VAH 48 and MLM 134 (Fig. 3a–c) are augen gneisses collected from the west and east ends of the Nordfjord. In CL images, zircon crystals are mostly subhedral, and dominated by low-luminescent, oscillatory zoned cores surrounded by bright rims, tips or prisms. The cores define concordia ages of 1653 ± 8 Ma (n = 6, MSWD = 0.9), 1651 ± 7 Ma (n = 9, MSWD = 1.6), 1621 ± 8 Ma (n = 5, MSWD = 1.2) respectively (Fig. 3a-c), recording the crystallization time of the granitic protolith. These samples have slightly depleted Hf isotopic compositions with mean εHf(t) values of +2.3 ± 0.8 to +3.1 ± 0.7, and highly elevated mean $\delta^{18}O$ values of 8.4–9.1‰.

4.3.2. Sveconorwegian (ca. 970–940 Ma) granitoids

Sample TSG-3 is taken from a foliated granite pluton in the Gulen dome. The granite grades into dioritic compositions towards the margins of the intrusion. Along the contact between the granite and the host rock, there is a zone of gneissic rocks that partly preserve granulite-facies mineral assemblages (Røhr et al., 2004). It is a weakly sheared biotite-rich granite (Fig. 3d). Zircon crystals are generally subhedral, 150–300 μm long, with aspect ratios of about 2. In CL images, most grains show moderately- to strongly-luminescent oscillatory zones. Twenty-five analyses define a concordia age at 966 ± 4 Ma (MSWD = 0.99) (Fig. 3d), representing the crystallization age of the sample. Sixteen analyses of zoned domains give an average εHf(t) value of −2.5 ± 0.5, and an average $\delta^{18}O$ value of 5.8 ± 0.2‰.

Two granitic samples (VAH 11, VAH 04) were collected from the inner Nordfjord, and sample VAH23 (Fig. 3e–g) was from the western end of the Nordfjord. Zircon grains from these samples are euhedral to subhedral, 150–250 μm long, with aspect ratios of about 2. They are dominated by oscillatory, banded or sector zones in CL images. The analyses on VAH 11, VAH 04 and VAH 23 give concordia ages of 961 ± 8 Ma (n = 12, MSWD = 1.7), 958 ± 7 Ma (n = 11, MSWD = 1.2), and 944 ± 7 Ma (n = 14, MSWD = 1.4) respectively (Fig. 3e–g). These ages are interpreted to record the time of crystallization of the granites. The first two samples, VAH 11 and VAH 04, have very similar Hf–O isotopic compositions, with significantly negative εHf(t) values (−5.1 ± 0.6 and −5.3 ± 1.0) and moderately elevated $\delta^{18}O$ values (6.8 ± 0.3‰ and 6.8 ± 0.2‰). Sample VAH 23 has an average εHf(t) value of −3.1 ± 0.7, and an average $\delta^{18}O$ values of 6.4 ± 0.4‰.

4.4. Synopsis of U–Pb, Lu–Hf and O isotope data

The geochronological data in this study include four igneous age groups of Gothian (1650–1620 Ma) and Telemarkian (1520–1500 Ma) metagranitoids and Sveconorwegian (1050–1020 Ma, 980–930 Ma) intrusions (Fig. 5a). The 1650–1620 Ma granitic rocks from the WGR are characterized by highly elevated $\delta^{18}O$ values of 8–9‰ associated with slightly positive Hf isotopic values of +2–+3. In contrast, the 1520–1500 Ma tonalitic and granitic rocks from the Hardangerfjord area and the Øygarden Complex show bimodal O isotopic charateristics; tonalitic rocks yield mantle-like O isotopic values while the granitic sample has a heavy $\delta^{18}O$ value of 8–9‰ (Fig. 6a). They all have significantly positive average εHf(t) values of +4–+7, more radiogenic than the Gothian samples. Six ca. 1050 Ma mafic and granitic rocks have very homogeneous and similar Hf–O isotopic compositions: the average εHf(t) values are −1–+2 and $\delta^{18}O$ values 6–6.5‰, while two ca. 1020 Ma leucogranite samples show a more evolved εHf(t) value of −3 to −2. The 980–930 Ma granites from the Hardangerfjord area and the Øygarden Complex have a relatively wide spread of εHf(t) values of −3–+3 and $\delta^{18}O$ values of 5.5–6.5‰, and 970–940 Ma granites from the WGR commonly have negative εHf(t) values of −5 to −3.

5. Results, migmatites

Key information on the migmatite samples is summarized in Table 2.

5.1. Hardangerfjord area

Two migmatite samples, H-01 and H-02 were taken several kilometers away from the Hardangerfjord shear zone. Sample H-01 is taken from a migmatitic dioritic gneiss with small stromatic and dilatational leucosomes that formed during shear deformation. The sampled domain is a foliation-parallel, medium grained, hornblende-bearing tonalitic leucosome (Fig. 4a). Zircon grains from this sample are subhedral to rounded with clear oscillatory zoning in dominant domains surrounded by CL-dark, unzoned rims. Seven analyses on cores define a concordia age of 1498 ± 10 Ma (MSWD = 1.8), representing the crystallization age of the dioritic protolith. Seven analyses on rims show a large scatter from ca. 1460 Ma to Cambrian times, and one nearly concordant spot has an age of ca. 1000 Ma (Fig. 4a). It is not possible to extract a reliable age of migmatitization from the data.

Sample H-02 is from the migmatitized part of a metavolcanic sequence in the 1.5 Ga Ullensvang group (Kinnsarvik formation; Sigmond, 1998). The sample is taken from a m-scale, medium- to coarse-grained tonalitic vein that fills a boudin-neck in between boudins of amphibolite (Fig. 4b). Zircon grains from this sample are elongated with round terminations. Most grains are entirely dark in CL, some have CL-bright cores with oscillatory/banded zones. Three analyses on cores are (nearly) concordant, with two of them yielding $^{207}Pb/^{206}Pb$ ages at ca. 1490–1470 Ma and the third one at ca. 1045 Ma (Fig. 4b). Eleven analyses on CL-dark domains are mostly discordant and show a scatter in apparent ages, ranging from Mesoproterozoic to Cambrian times. Five concordant or nearly concordant analyses yield a $^{206}Pb/^{238}U$ age at 600–0 Ma. The scatter is probably attributed to variable Caledonian lead loss due to metamictization. Collectively, the data suggest formation of the volcanic protolith at ca. 1490–1470 Ma, possible migmatitization and vein formation at ca. 1045 Ma and a final event of Caledonian lead loss.

5.2. Øygarden Complex

Migmatites in the Øygarden Complex contain moderate to high volumes of leucosomes, forming regularly metatexites and sometimes diatexites. They are usually of granitic composition but host abundant mafic bodies. In places, quartzite and mica-schist are associated with the migmatites. This suggests that at least part of the migmatites formed through melting of metasedimentary protoliths. The entire complex experienced strong penetrative shear deformation during late Caledonian collapse (Wiest et al., 2020a). Therefore, pre-Caledonian relationships have been obliterated except for low-strain domains, which represent the targets of this study.

Sample ØC-01 is a granitic diatexite that contains blocks of amphibolite and quartzite (Fig. 4c). The sampled domain is a coarse-grained hornblende-bearing granitic leucosome. In CL images, most zircon grains show cores with fine oscillatory zoning surrounded by CL-bright mantles with faint oscillatory or banded zones and dark, unzoned rims (Fig. 4j). The size of mantle and rim domains varies between different crystals. Core domains show zircon inheritance from the protolith of the migmatite, with 3 of them yielding a concordia age at 1640 ± 9 Ma (MSWD = 1.4) while others are highly discordant. The age from oscillatory zoned mantles is similar to that of the CL-dark rims. The dark rims are all characterized by a low Th content (3–13 ppm) and therefore a low Th/U ratio (≤0.01). Ten analyses in the mantles and rims define a common concordia age at 1043 ± 6 Ma (MSWD = 1.18), which represents the time of crystallization of the leucosomes (Fig. 4c). Two analyses on mantle and rims have distinctly higher Th concentration and Th/U ratio, and are concordant at ca. 925 Ma and ca. 650 Ma respectively, which may be a result of incomplete Pb loss during Caledonian

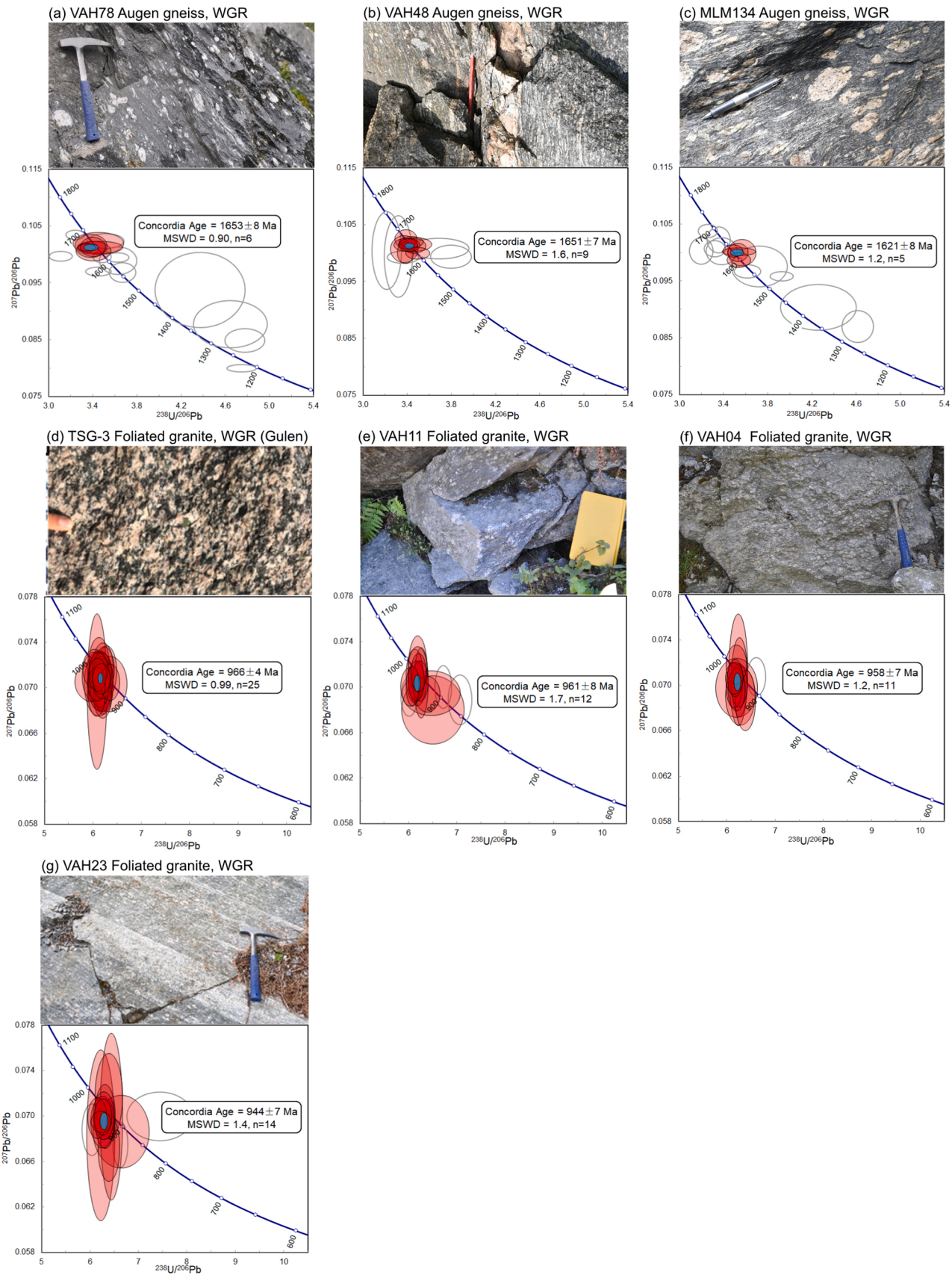

Fig. 3. Field outcrop photographs and zircon U–Pb Tera-Wasserburg diagrams of igneous samples from the WGR; Same as the caption to Fig. 2. For details of each data-point see Table 1, Supplementary File B.

Table 2
Summary of U-Pb geochronology and Hf isotopic results of leucosome samples in this study.

Sample	Longitude (E)	Latitude (N)	Rock types	Mineral composition	Protolith age	Migmatization age	εHf(t) of anatectic zircons
H-01	6.28502	60.15316	Tonalitic leucosome in metatexite	Qz + Pl + Kfs + Bt + Spn	1498 ± 10 Ma		
H-02	6.37713	60.19363	Tonalitic leucosome in metatexite	Qz + Pl + Kfs + Bt	ca. 1500 Ma		
ØC-01	4.81128	60.63487	Granitic leucosome in diatexite migmatite	Qz + Kfs + Pl + Bt + Ep	1640 ± 9 Ma	1043 ± 6 Ma	−2.2 ± 1.3
ØC-03	4.91911	60.45208	Tonalitic leucosome in metatexite	Qz + Pl + Amp + Bt + Spn + Ep	1491 ± 8 Ma	1090–970 Ma	
ØC-05	4.94171	60.48861	Tonalitic leucosome in metatexite	Qz + Pl + Bt + Ms	ca. 1600 Ma, 1480 ± 9 Ma	1034 ± 5 Ma	−4.0 ± 1.7
ØC-07	4.79851	60.55249	Granitic veins intruding boudinaged amphibolite	Qz + Kfs + Pl + Bt + Spn + Ep		1030 ± 4 Ma	−4.2 ± 0.7
GU-01	5.09126	60.84787	Granitic leucosome in metatexite	Qz + Kfs + Pl + Bt + Ep + Spn	1492 ± 11 Ma, 1419 ± 13 Ma	1053 ± 12 Ma, 1014 ± 6 Ma	−2.8 ± 1.5
GU-02	5.06695	60.87438	Granitic leucosome in metatexite	Qz + Kfs + Pl + Bt + Ms + Ep + Spn		1050–940 Ma	−6.2 ± 1.4
GU-03	5.02634	60.93123	Granitic leucosome in metatexite	Qz + Kfs + Pl + Bt + Ep	ca. 1600 Ma	1052 ± 6 Ma	−4.5 ± 1.3

thermal events. The older cores generally have positive εHf(t) values of +2–+4, while the ca. 1043 Ma domains have an average εHf(t) value of −2.2 ± 1.3 (n = 8).

Sample ØC-03 is a granitic metatexite with thin and folded stromatic leucosomes and larger patches of melt. The sample is a coarse-grained hornblende-bearing granitic leucosome (Fig. 4d). Zircon grains show moderate CL luminosity with fine oscillatory zones partly surrounded by CL-darker, unzoned or faintly zoned rims. Eight analyses on oscillatory-zoned domains with typical Th/U ratios of igneous zircons (0.34–0.72) show similar ages and 5 of them give a concordia age at 1491 ± 8 Ma (MSWD = 1.6), representing the single-sourced zircon inheritance from the protolith. By comparison, the rims commonly have higher U (560–2110 ppm), lower Th (10–140 ppm) and Th/U ratios (0.02–0.14). The $^{206}Pb/^{238}U$ ages of 9 analyses range from 1088 Ma to 972 Ma ($^{206}Pb/^{238}U$ ages, Fig. 4d), probably indicating zircon recrystallization/regrowth during a long-term thermal event.

Sample ØC-05 is a granodioritic metatexite with thin, ptygmatically folded leucosomes and locally diffuse, coarser-grained patches (Fig. 4e). The leucosomes are surrounded by thin biotite melanosomes. The sample is a coarse-grained granitic leucosome patch. Zircon grains are partly small and stubby (<100 μm) with CL-dark rims around zoned cores, and partly elongated (150–300 μm long) with oscillating/banded zones (Fig. 4k). Four analyses on the cores of the former give a concordia age at 1480 ± 9 Ma (MSWD = 0.61), and the remaining one is older at ca. 1600 Ma (Fig. 4e). A concordia age at 1034 ± 5 Ma (MSWD = 1.5) is defined by 8 concordant analyses on each rim and the zoned domains (Fig. 4e), representing the time of crystallization of the leucocratic vein. The older cores generally have positive εHf(t) values of +2–+6; three analyses on ca. 1034 Ma domains have an average εHf(t) value of −4.0 ± 1.7, while two yield a slightly positive value of 0–+2.

Sample ØC-07 is taken from within a K-feldspar-rich leucogranite body that is unfoliated. The leucogranite itself is very homogeneous and consists almost entirely of feldspar and quartz. However, it contains numerous mafic bodies that occur as m-scale dykes, aligned (but disconnected) patches, up to 20 m long schlieren or isolated irregularly shaped blobs. Granitic veins, rooted in the leucogranite, commonly intrude the mafic bodies. In places, the mafic bodies developed a solid-state foliation parallel to their outer perimeter that is cut by the granitic veins. The contact relationships suggest that the mafic melt was injected into the granite body while the latter was close to its crystallization temperature. This led to a remobilization of granitic melt that intruded the mafic bodies, which were already solid because of their higher solidus temperature. The sample was taken from coarse-grained granitic veins (Fig. 4f) that cut through foliated amphibolite. Zircon grains from this sample are euhedral to subhedral, and are weakly to moderately luminescent with clear oscillatory zones in CL images. The crystallization age is determined by the concordia age of 15 analyses at 1030 ± 4 Ma (MSWD = 1.3) (Fig. 4f). Fifteen analyses yield a homogeneous Hf isotopic composition, with an average εHf(t) value of −4.2 ± 0.7.

5.3. Southern Western Gneiss Region, Gulen area

The migmatites from the Gulen area commonly show a high degree of migmatization with a large volume of leucosomes. Like in the Øygarden Complex, quartzites and mica schists are found locally contained within migmatites and witness a metasedimentary protolith. During the Caledonian orogeny, mafic bodies within the migmatites have been transformed to eclogite, while the migmatites themselves appear unaffected by this metamorphism (Wiest et al., 2019). However, large volumes of the migmatites have been strongly deformed during extensional collapse of the Caledonian orogen. The samples were taken from domains that escaped Caledonian shear deformation.

Sample GU-01 is a granitic metatexite preserved in sheared gneisses in the footwall of the Bergen Arcs shear zone. Leucosomes occur as stromatic layers and as diffuse patches (Fig. 4g). The sampled domain is a medium-grained patch of granitic composition. Zircon grains from this sample are 150–250 μm long with roundish terminations, composed of oscillatory-zoned cores and CL-dark, wide rims. Some crystals also have strongly luminescent mantles (Fig. 4n). The analyses on cores define two groups of concordia ages at 1492 ± 11 Ma (MSWD = 0.81, n = 4) and 1419 ± 13 Ma (MSWD = 1.5, n = 2) respectively, which are interpreted as inherited zircons. Two concordia ages at 1053 ± 12 Ma (MSWD = 1.6, n = 3) and 1014 ± 6 Ma (MSWD = 1.9, n = 4) are defined by analyses on CL-bright mantles and rims (Fig. 4g). These two ages likely indicate two episodes of zircon recrystallization and/or overgrowth during metamorphism and migmatization, or reflect a protracted thermal event lasting for 40 Ma. An alternative possibility, although not preferred here, is they represent incomplete lead-loss, with the two ages capturing a snapshot of a lead-loss trend to a young Sveconorwegian age. Five analyses on mantle/rim domains yield εHf(t) value of −5–0 with an average εHf(t) value of −2.8 ± 1.5.

Sample GU-02 is a veined granitic metatexite that experienced weak penetrative shear deformation. The sampled domain is a coarse-grained granitic leucosome (Fig. 4h), which is surrounded by a biotite melanosome. Zircon grains from this sample are subhedral to elliptical with clear core-rim structures. The cores have euhedral to irregular shape and are relatively CL-bright with oscillatory zones, while the broad rims are CL-darker with banded, oscillatory or no zones (Fig. 4m). Three analyses on cores are slightly discordant, ranging in age from 1370 Ma to 1500 Ma ($^{207}Pb/^{206}Pb$ ages). Ten concordant analyses yield concordia ages of ca. 1050–940 Ma ($^{206}Pb/^{238}U$ ages), indicating zircon recrystallization/

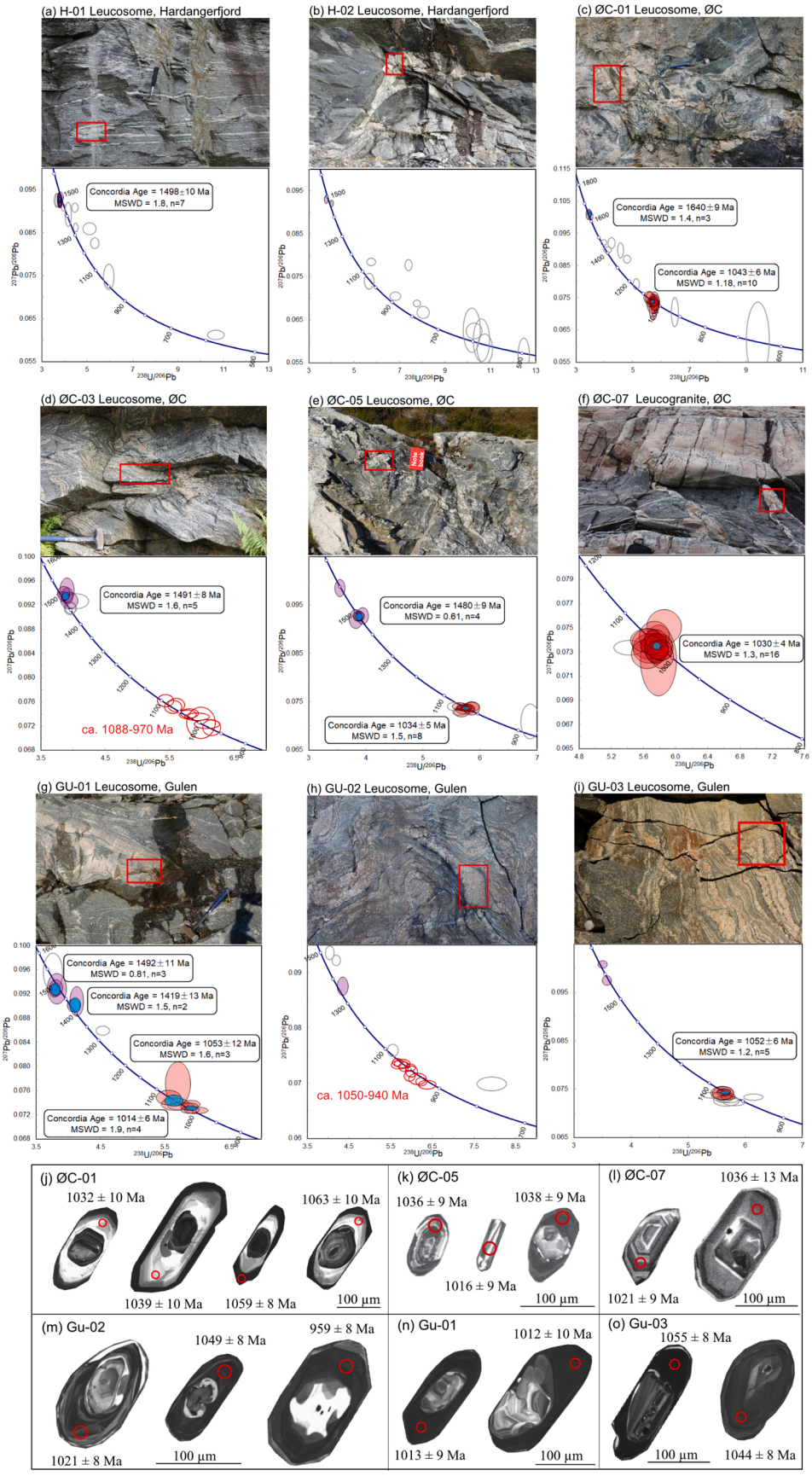

Fig. 4. Field photographs, zircon U–Pb Tera-Wasserburg diagrams and CL images for migmatite samples in this study. red ellipses: anatectic zircons used for calculation of concordia age (filled) and represeting a wider range of ages (open); purple: protolith zircons; grey: (reversely) discordant and Pb-loss analyses. For details of each data-point see Table 2, Supplementary File B. The red rectangles on field photos show sampling location of leucosomes.

regrowth during long-term high-grade metamorphism and migmatization. Five analyses on ca. 1030–950 rims yield εHf(t) values of –8 to –4 with an average εHf(t) value of −6.2 ± 1.4.

Sample GU-03 is a weakly deformed granitic metatexite. Amphibolite layers within the migmatite have been statically transformed into eclogite during the Caledonian orogeny. The migmatite contains stromatic and vein leucosomes that are surrounded by biotite melanosomes (Fig. 4i). The sampled domain is a coarse-grained patch of granitic leucosome. This sample has subhedral to rounded zircon grains with wide, CL-dark rims around irregular cores (Fig. 4o); some grains are almost entirely oscillatory/banded-zoned with very small cores. Two nearly concordant analyses on cores have ages at ca. 1580 Ma and ca. 1640 Ma, respectively. Ten analyses on zoned grains and rims give very similar ages, suggesting that crystallization of new zircon occurred at the same time that the CL-dark zircon rims grew. Five of them define a concordia age of 1052 ± 6 Ma (MSWD = 1.2) (Fig. 4i). This age is interpreted as the time of crystallization of the leucocratic vein. Six analyses on ca. 1052 Ma domains give an average εHf(t) value of −4.5 ± 1.3.

5.4. Summary of zircon U-Pb geochronology and Hf isotopic composition

In summary, zircon grains from the dated leucosomes generally display two kinds of internal structures in CL images. One has oscillatory- or banded- zoned cores enveloped by CL-bright or -dark rims that are structureless or have faint zoning. The second one shows euhedral prismatic zircons with oscillatory zoning (Fig. 4j–o). The core domains generally have relatively low U concentrations and Th/U ratios >0.1, which display Gothian and Telemarkian (1650–1500 Ma) ages and represent primary igneous zircons. In contrast, the simply zoned grains and zircon rims mostly have much higher U contents and lower Th/U ratios, which have a wide range of age between 1050 and 950 Ma and yield a peak at ca. 1030 Ma (Fig. 5b, c). This is coeval with the igneous crystallization age of the leucogranite sample (ØC-07) and is interpreted to represent the timing of high-grade metamorphism and migmatization. The zircons from the leucosomes and leucogranite samples commonly have an enriched Hf isotopic composition with εHf(t) values mostly of −6 to −3, in contrast to the ca. 1050 Ma igneous samples, which generally have an averaged positive εHf(t) value (Fig. 6b).

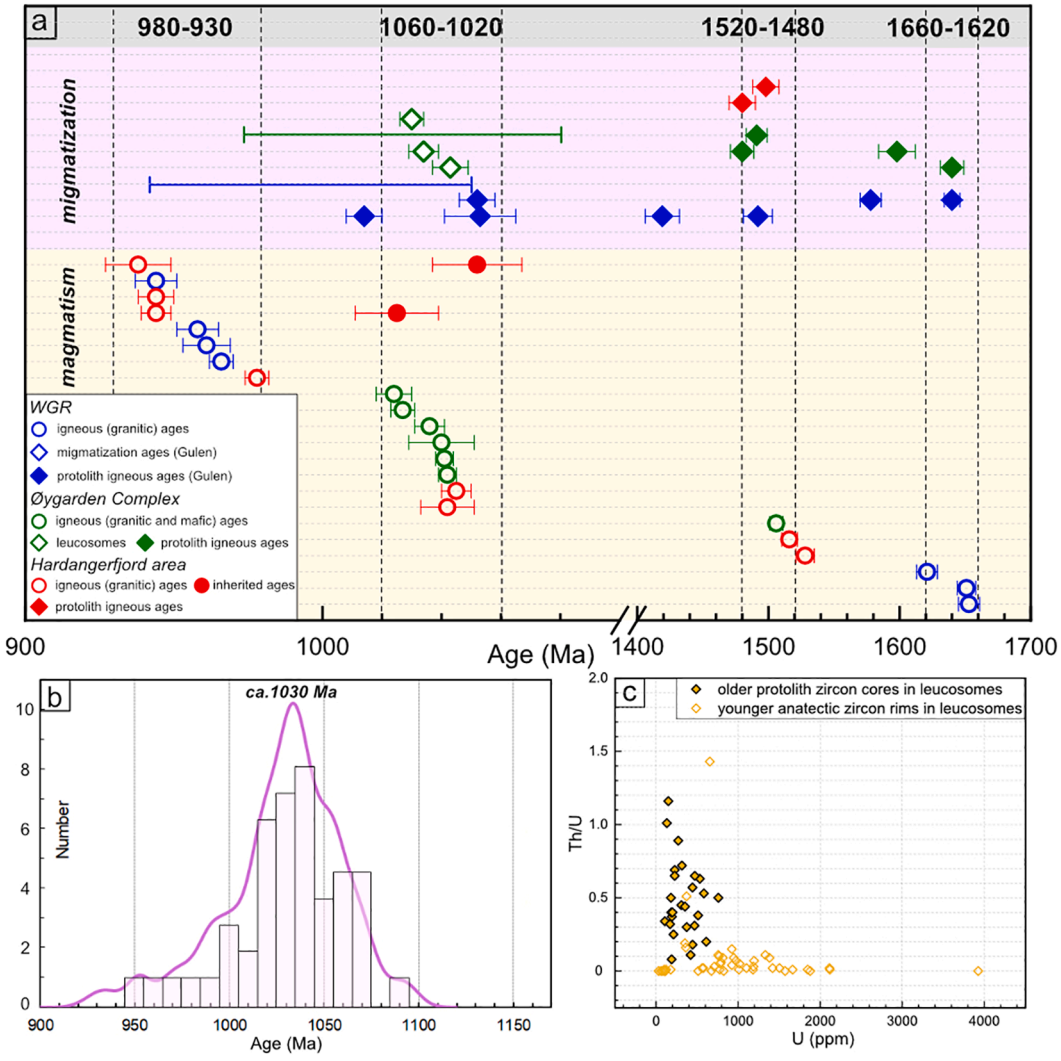

Fig. 5. (a) Summary of magmatic and migmatitic ages in the study areas including ages from Wiest et al. (2018), with dash lines showing the main magmatic periods. The two lines on the top indicate long-lasting or repeated migmatization of samples ØC-03 and GU-02. (b) Histogram and probability distribution of U-Pb ages of zircons from leucosomes; the age peak at ca. 1030 Ma probably indicates the climax of high-grade metamorphism and migmatization; (c) U versus Th/U ratio of dated zircon domains from the leucosomes, showing that older cores and younger mantles/rims have distinct Th/U signatures.

6. Discussion

6.1. Geochronology: Magmatism and migmatization

The new zircon U–Pb ages obtained in this study range from ca. 1650 to 930 Ma and demonstrate the importance of the Sveconorwegian records in the Baltican basement of the southern Scandinavian Caledonides. These results make it possible to link the 'Caledonized' basement to well-established Sveconorwegian Province in the (western) Sveconorwegian lithotectonic units.

6.1.1. Gothian (ca. 1650 Ma) vs. Telemarkian (ca. 1500 Ma) crust

As outlined above, the age of the first (oldest) lithosphere formation in each lithotectonic unit of the Sveconorwegian orogen decreases in a stepwise fashion towards the west: Transcandinavian Igneous Belt (1710–1660 Ma) in the Eastern Segment, Gothian (1660–1520 Ma) in the Idefjorden, Bamble and Kongsberg units, and Telemarkian (1520–1480 Ma) in the Telemarkia unit (Bingen et al., 2005). The data from the studied areas can be correlated to Gothian and Telemarkian crust.

In the Hardangerfjord area, two samples of tonalitic gneiss yield ages of ca. 1520 Ma and four samples of migmatite and granite host have 1500–1470 Ma inherited zircons. These results largely confirm previously reported geochronological data from the Hardangerfjord area (Bingen et al., 2005; Roberts et al., 2013). They support a Telemarkian age of the crust formation in the area and suggest that large parts of the Hardangerfjord area belong to the Telemarkian Suldal volcanic arc (Roberts et al., 2013). In the Øygarden Complex, Telemarkian granitic gneisses (ca. 1506 Ma) are also found (Wiest et al., 2018) as well as inherited zircon cores between ca. 1490 and 1480 Ma in migmatites. Two samples though (ØC-01 and ØC-05), contain Gothian zircon populations (1640–1600 Ma). In the Gulen area of the southern WGR, migmatite samples similarly contain Telemarkian (ca. 1500–1490 Ma) in addition to Gothian (ca. 1640 Ma) inherited zircon populations. Elsewhere in the WGR, the oldest orthogneiss protoliths are Gothian with ages ranging from ca. 1650 to 1620 Ma (3 samples of this study and published data; Austrheim et al., 2003; Corfu et al., 2014b; Krogh et al., 2011; Røhr et al., 2013), while Telemarkian ages are absent.

Collectively, the data suggest that the Øygarden and Gulen areas represent a transition zone between Telemarkian crust in the southwest and Gothian crust in the northeast, with no mappable discrete boundary as proposed by Roffeis et al. (2013).

6.1.2. Sveconorwegian (1060–1020 Ma) magmatism and migmatization

The Sirdal Magmatic Belt (SMB) is a large composite batholith formed between ca. 1060 and 1020 Ma in South Norway (Coint et al., 2015; Slagstad et al., 2013). Its formation was accompanied and followed by regional granulite-facies metamorphism between ca. 1045 and 990 Ma (Bingen et al., 2008a; Drüppel et al., 2013; Blereau et al., 2017; Laurent et al., 2018a,b; Slagstad et al., 2018b). Based on the recognition of 1050–1020 Ma granitic and gabbroic magmatism in the Øygarden Complex, Wiest et al. (2018) concluded that the SMB continues towards the NNW into the Caledonian province. While this has been reaffirmed by additional dating of granites in the Øygarden Complex (sample TSS-2, ca. 1036 Ma) and geophysical correlations with the SMB (Slagstad et al., 2018a), no evidence from the interjacent Hardangerfjord area was previously available. Two of our samples of foliated/gneissic K-feldspar megacrystic granite-granodiorite (HCT-5, 1045 ± 5 Ma and HCT-16, 1042 ± 9 Ma) document 1050–1020 Ma felsic magmatism in the Hardangerfjord area for the first time and thereby establish the missing link between the autochthonous basement windows in the Caledonian province and the Sveconorwegian province. This indicates that 1060–1020 Ma magmatism occurred in a distinctly NNW-trending, ca. 300 km long magmatic belt. Within this domain, it appears that the emplaced magmas decrease in volume from south to north until they disappear in the southern WGR.

Furthermore, our new data document a temporal and spatial association between 1050 and 1020 Ma magmatism and migmatization in the Hardangerfjord area, the Øygarden Complex and the southern WGR. The ages of migmatization are constrained by dating of zircon grains and rims from leucosomes. Nine samples of migmatite show a wide range of concordant ages, which encompasses almost the entire range of Sveconorwegian magmatism from 1050 to 950 Ma. However, the majority of ages falls between 1050 and 1020 Ma, which is coeval with SMB-type magmatism (Fig. 5). The relative probability distribution of migmatite ages shows a prominent peak at ca. 1030 Ma, which conforms to the magmatic crystallization age of the leucogranite sample (ØC-07) that apparently represents the climax of high-grade metamorphism and crustal anatexis. This age falls in between two distinct magmatic pulses in the Øygarden Complex, namely a pulse of mafic to intermediate magmatism at ca. 1040 Ma, and a pulse of leucogranite magmatism at ca. 1020 Ma (Wiest et al., 2018). The clear temporal and spatial link between migmatization and magmatism supports the interpretation from the Rogaland area in southwest Norway, that mafic magmatism and underplating were driving migmatization in the crust (Laurent et al., 2018a; Slagstad et al., 2018b).

In contrast to previous studies, our results demonstrate that the southernmost part of the WGR (Gulen area) was affected by migmatization between ca. 1050 and 1020 Ma, in a time interval overlapping with intrusion of the SMB. So far, all previously reported ages of Sveconorwegian migmatites and high-grade metamorphism in the WGR are younger than 1000 Ma (Skår and Pedersen, 2003; Røhr et al., 2004, 2013; Kylander-Clark and Hacker, 2014). While the Proterozoic evolution of most parts of the WGR is still poorly constrained, the currently available data suggest that the Øygarden and Gulen areas represent a gradual western boundary of pre-1000 Ma tectono-magmatic activity in the Sveconorwegian orogen. As mentioned before, this coincides with the gradual transition from Gothian to Telemarkian crust.

6.1.3. Late-Sveconorwegian (980–930 Ma) magmatism and migmatization

Plutons of the hornblende-biotite granite (HBG) suite formed between 980 and 930 Ma over most of the Sveconorwegian orogen in South Norway (Bogaerts et al., 2003; Vander Auwera et al., 2011; Granseth et al., 2020). In the studied areas, late-Sveconorwegian plutons are common: four of them are dated between c. 978 and 938 Ma in the Hardangerfjord area, and another four of them between c. 966 and 943 Ma in the WGR (Table 1). In the Øygarden Complex, sample ØC-03 shows evidence for protracted zircon growth during migmatization until ca. 970 Ma, however, no pluton of this age group is exposed.

In the Hardangerfjord area, the conspicuous feature of the late-Sveconorwegian plutons is an almost perfectly circular shape with little to no deformational fabric. A *syn*-magmatic foliation is visible at the margin of the plutons (e.g. samples HCT-3 and HCT-12) and a Caledonian fabric may only be locally present. In the WGR, in contrast, these plutons have been variably deformed into elliptical bodies and can thus serve as strain markers. In the Gulen area, sample TSG-3 robustly constrains the age of a ca. 25 × 10 km large pluton at ca. 966 Ma. This pluton is deformed and reworked along several Caledonian shear zones (Wiest et al., 2019). This age of c. 966 Ma is identical within errors with U–Pb zircon and monazite ages of granulite-facies rocks (Røhr et al., 2004), which occur along the rim of the pluton, where the granite grades into monzonitic and dioritic compositions (Wiest et al., 2019). The range of ages in the nearby migmatite samples suggests that the granite intruded a long-lasting migmatite terrane that was around or above solidus conditions for almost 100 Myrs (between ca. 1050 and 950 Ma). Therefore, it seems likely that granulite facies conditions in the Gulen area developed locally in the thermal aureole of the pluton. However, the regional occurrence of Sveconorwegian granulite-facies metamorphism, i.e. also in other parts of the WGR (Engvik et al., 2000; Krabbendam et al., 2000), makes the mechanism of metamorphism and its relations to magmatism speculative.

6.1.4. Caledonian vs. Sveconorwegian reconstructions

Our results confirm that U-Pb zircon geochronology allows to disentangle Sveconorwegian magmatism and migmatization from the effects of Caledonian reworking in the Baltican basement, in accordance with previous studies (Røhr et al., 2013; Kylander-Clark and Hacker, 2014; Wiest et al., 2018). The intersection of two orogenic belts poses challenges but it also allows chances to gain insights into the evolution of both orogens.

A remaining challenge is the unequivocal identification of Caledonian versus Sveconorwegian migmatitization in the Baltican basement windows. The spatial distribution of the two generations of migmatites has proven highly variable (Gordon et al., 2013, 2016; Kylander-Clark and Hacker, 2014; Wiest et al., 2021) and remains unclear for large parts of the WGR, due to the lack of high-precision in-situ dating. This is a major drawback for orogenic reconstructions, since migmatites play a crucial role in orogen dynamics (Vanderhaeghe and Teyssier, 2001; Vanderhaeghe, 2012). Similarly, the NE boundary of Sveconorwegian reworking in the WGR, originally defined by Tucker et al. (1990), is poorly constrained. Furthermore, it is uncertain whether post-1000 Ma granites occur to the north of Nordfjord and the apparent absence of 1500–1000 Ma magmatism and migmatization in most parts of the WGR is an enigmatic issue that hampers reconstructions of the geodynamic setting and tectonic evolution of the Sveconorwegian orogen (Bingen et al., 2005, 2008a; Slagstad et al., 2013).

The complementary erosion levels of the Baltican crust in the Caledonian and Sveconorwegian provinces may provide important insights. In South Norway, mostly the upper parts of the Sveconorwegian orogen are exposed. Deep levels of the Sveconorwegian crust are only exposed in areas that were affected by intense late-/post-orogenic exhumation (Bingen et al., 2006) such as the Rogaland Igneous Complex (Slagstad et al., 2018b) and the Eastern Segment (Viola et al., 2011; Möller et al., 2015; Möller and Andersson, 2018). The Baltican basement windows of the Caledonides expose different sections of the Caledonian orogenic crust, due to the highly variable effects of Devonian post-orogenic collapse (Fossen, 2010). The Hardangerfjord shear zone (Fig. 1c) marks the southern limit of thick-skinned collapse-related deformation (Fossen et al., 2014) and the erosion level exposes consequently high levels of the Caledonian orogen. Due to variable crustal flow, the metamorphic core complexes along the coast of West Norway, in contrast, exhumed different levels of the crust (Andersen et al., 1994; Wiest et al., 2019). The Øygarden Complex, for example, exposes a ca. 10 km vertical (Caledonian) crustal section from localized shearing at upper levels to a Caledonian migmatite dome at the lowest levels (Wiest et al., 2020a). However, these distinct Caledonian structural levels coincide also with distinct Sveconorwegian lithologies, which comprise mostly plutons and supracrustal cover at upper structural levels and dominantly (Sveconorwegian) migmatites at lower levels. Possibly, the intense ductile flow in the WGR north of Nordfjord during Caledonian collapse (Labrousse et al., 2004; Wiest et al., 2021) resulted in the complete removal of the upper Sveconorwegian crust, while exposing the lower crust. This could explain why Sveconorwegian migmatites are abundant while plutons are rare.

Independent of this, our study demonstrates a significant influence of Sveconorwegian tectono-metamorphism on later tectonic episodes. The inferred boundary between Telemarkian and Gothian crust, which corresponds to the northern boundary of SMB magmatism, coincides with the northern Bergen Arcs Shear Zone (Wennberg et al., 1998), a Devonian extensional detachment. This suggests that crustal heterogeneities inherited from the Sveconorwegian orogeny affected the localization of Caledonian shear zones. Similarly, Jakob et al. (2019) suggested that inherited Sveconorwegian lineaments had a control on the development of the segmented pre-Caledonian passive margin of Baltica and thereby the architecture of Caledonian thrust nappes. Furthermore, outside of the Caledonian province, inherited Sveconorwegian structures played an important role for brittle reactivation during Permian-Mesozoic rifting (Sundvoll and Larsen, 1994; Scheiber et al., 2015).

6.2. Proterozoic crustal evolution revealed by U–Pb–Hf–O isotopes

In the recent decade, numerous geochronological and isotopic data of ca. 1.86–0.90 Ga rocks in Fennoscandia, in particular paired zircon U–Pb and Lu–Hf data, have been published (Fig. 8a). This has led to an improved understanding of crustal evolution and tectonics in relation to the amalgamation of supercontinents Columbia/Nuna and Rodinia. However, O isotopic characterization of zircon has been utilized to a much lesser degree so far. Existing combined zircon U–Pb, Lu–Hf and O isotopic data focus on the Telemarkian and Gothian rocks (e.g. Roberts et al., 2013; Petersson et al., 2015), whilst analyses of Sveconorwegian rocks are largely missing. In the following section, we discuss zircon Hf–O isotopic signatures of the two main age groups of ca. 1650–1500 Ma and 1050–930 Ma samples in this study and assess the origin and evolution of the Gothian, Telemarkian and Sveconorwegian rocks.

6.2.1. 1650–1500 Ma Gothian and Telemarkian crust

Three 1650–1620 Ma granitic gneiss samples of the Gothian crust from the WGR define the oldest samples in this study. They generally have radiogenic Hf isotopic compositions with positive εHf(t) values, but the εHf(t) values are >6 units below the DM reservoir vector (Fig. 6b). The Hf isotopic signature, coupled with highly elevated $\delta^{18}O$ values (8–9‰, Fig. 6a), is consistent with the involvement of older crust, and/or the addition of sedimentary components during the genesis of these granitic magmas, which were probably derived from inboard of Fennoscandia, such as the Svecofennian (1910–1750 Ma) and post-Svecofennian (1710–1660 Ma) crust.

Compared to the Gothian samples, the Hf isotopic compositions of 1520–1500 Ma tonalitic and granitic samples from the Hardangerfjord area and the Øygarden Complex are more radiogenic with εHf(t) values of +3 to +8 (Fig. 6b), indicating an increasing juvenile input and decreasing crustal reworking. Their O isotopes in this study exhibit bimodal characteristics, with the $\delta^{18}O$ values of two tonalitic samples in the range of and slightly below the mantle value while that of a granitic sample being significantly high ($\delta^{18}O$ = 8–9‰); the Hf isotopes of the former are slightly more radiogenic than the latter (Fig. 6a). In the adjacent Suldal area to the south, a large spread of Hf and O isotope compositions of 1520–1480 Ma granitoids (Suldal volcanic arc) has been reported with εHf(t) and $\delta^{18}O$ values of +1 to +11 and 6–8‰ respectively; the Hf and O isotopic values have a broadly negative correlation and the samples were interpreted to have derived from a mixture of enriched mantle with moderately elevated $\delta^{18}O$ values and high-$\delta^{18}O$ sedimentary components (Roberts et al., 2013). The O isotope values of two tonalitic gneisses in this study (HCT-11, HCT-13, ca. 4.5‰) are slightly lower than mantle values, indicating a possible assimilation of hydrothermally altered rocks by isotopically light meteoric water during the formation of the tonalitic magmas, which is not uncommon in a subduction-related arc setting (Troch et al., 2020).

We compiled the Hf–O isotopic results of our samples with available published data from the Sveconorwegian orogen (Fig. 8). These data clearly show that the Telemarkian and pre-Telemarkian crust (1800–1480 Ma) is mostly characterized by juvenile Hf isotopic compositions with positive εHf(t) values. The post-1600 Ma Gothian and Telemarkian rocks generally have considerably more juvenile Hf isotopic compositions than the Paleoproterozoic crust and varying $\delta^{18}O$ values in a wide range of 4.5–9‰, which was probably related to the tectonic switching between advancing and retreating subduction along the long-lived active continental margin of Fennoscandia with more juvenile input and a large volume of sedimentary material involved (Roberts and Slagstad, 2015; Petersson et al., 2015).

6.2.2. 1050–930 Ma Sveconorwegian crust

Although only a small volume of ca. 1050 Ma mafic rocks is exposed in the SMB, a number of previous studies agree that the underplating of mafic magmas could have occurred extensively and constitute an important composition of the lower continental crust in this region

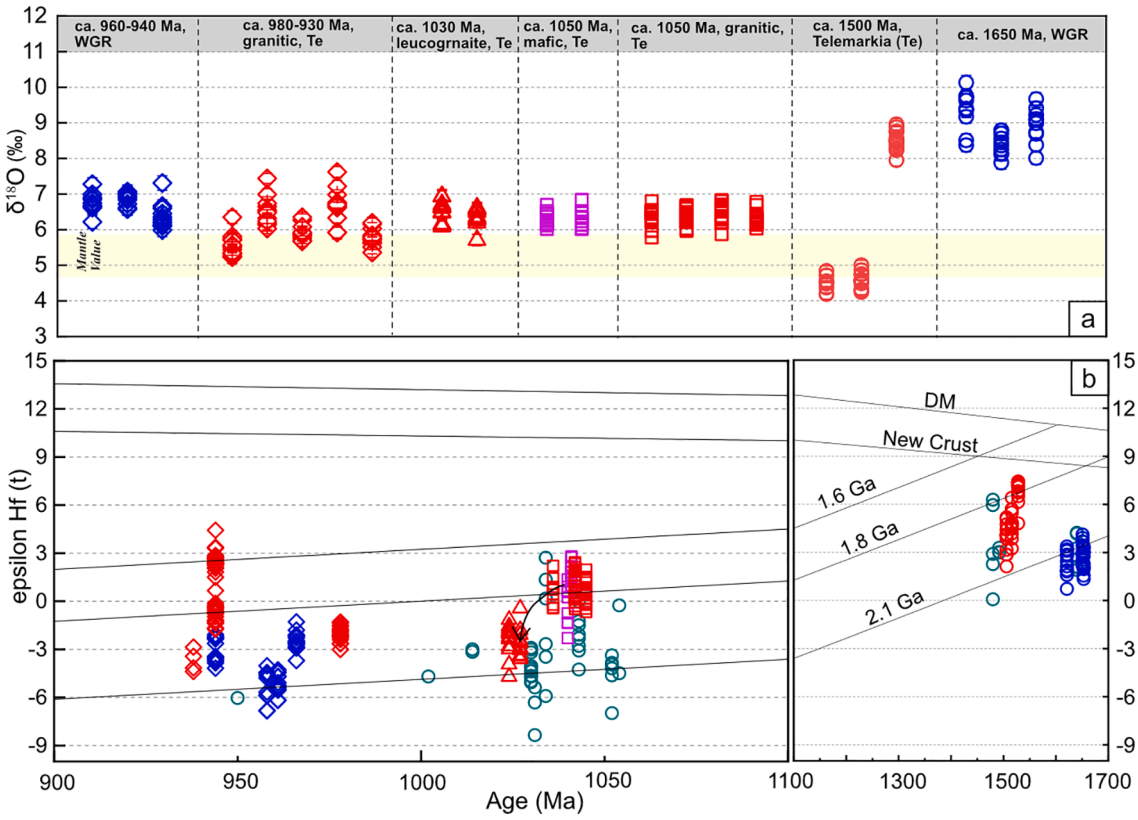

Fig. 6. (a) O isotope composition of the samples in this study, with age, lithologies and locations marked on the top. Te, Telemarkia unit; (b) Initial epsilon Hf values versus crystallisation ages of the samples analyzed in this study; The evolution curves of the depleted mantle (DM) and the new crust are from Griffin et al. (2000) and Dhuime et al. (2011) respectively. The legend is the same as for (a), and the green open circles indicate the zircons from the leucosomes. The black arrow shows the variation of εHf(t) values from ca. 1050 Ma to ca. 1020 Ma.

(Bybee et al., 2014; Slagstad et al., 2018b; Bingen et al., 2021). These underplated mafic magmas were believed to have provided the heat for the generation of granites, however, their origin and the relationships with coeval granites remain poorly understood due to a lack of geochemical and isotopic constraints. In this study, the ca. 1050 Ma mafic samples (gabbro and amphibolite from Wiest et al., 2018) have

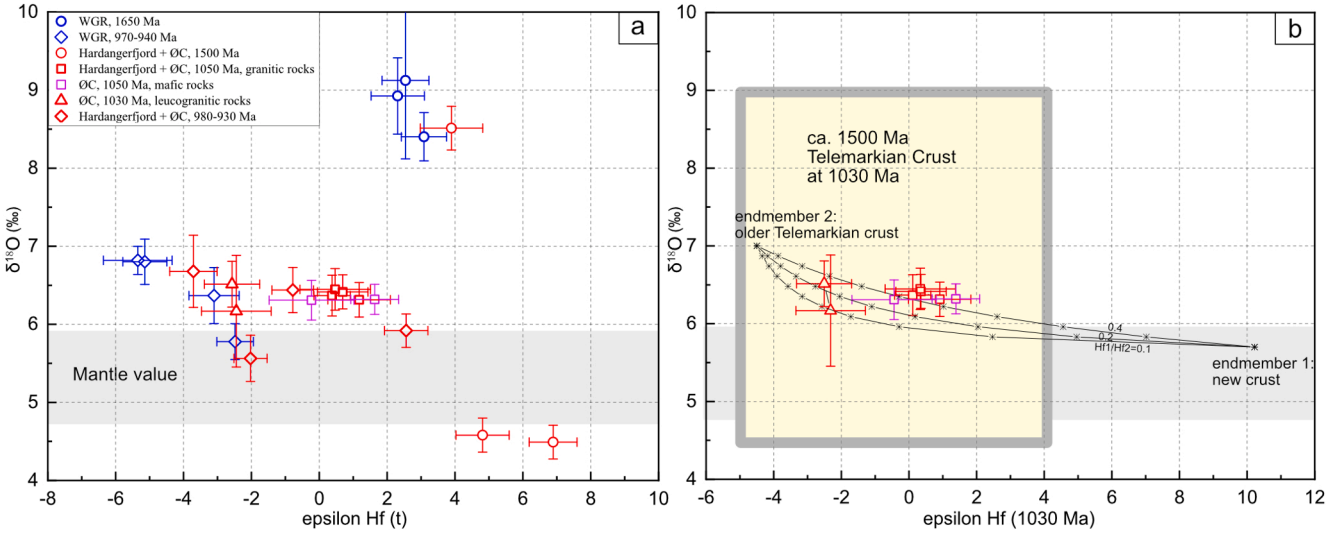

Fig. 7. (a) Initial epsilon Hf versus $\delta^{18}O$ values of all samples in this study; (b) Mixing between a new crustal component (endmember 1) and an older crustal component (endmember 2), showing Hf-O isotopic signatures of ca. 1050–1020 Ma samples (see text for details), with ticks representing 10% mixing. All εHf values of samples and endmembers are recalculated to 1030 Ma. An εHf value of − 4.5, which is consistent with the Hf isotopic composition of the ca. 1030 Ma leucogranite sample ØC-07 (average εHf(t) = −4.2 ± 0.7), is assumed for the average Hf isotopic values of ca. 1.5 Ga Telemarkian crust at ca. 1030 Ma. A moderately elevated value of 7‰ is used to represent the average O isotopic compositions of the older crustal endmember. The new crust is assumed to have εHf = +10.2 at ca. 1030 Ma (Dhuime et al., 2011), and its $\delta^{18}O$ value is assumed to be 5.7‰. Hf-concentration ratios between endmembers 1 and 2 are set at 0.1, 0.2 and 0.4 (Rudnick and Gao, 2003). The rectangle shows the Hf and O isotopic range of the Telemarkian crust at ca. 1030 Ma.

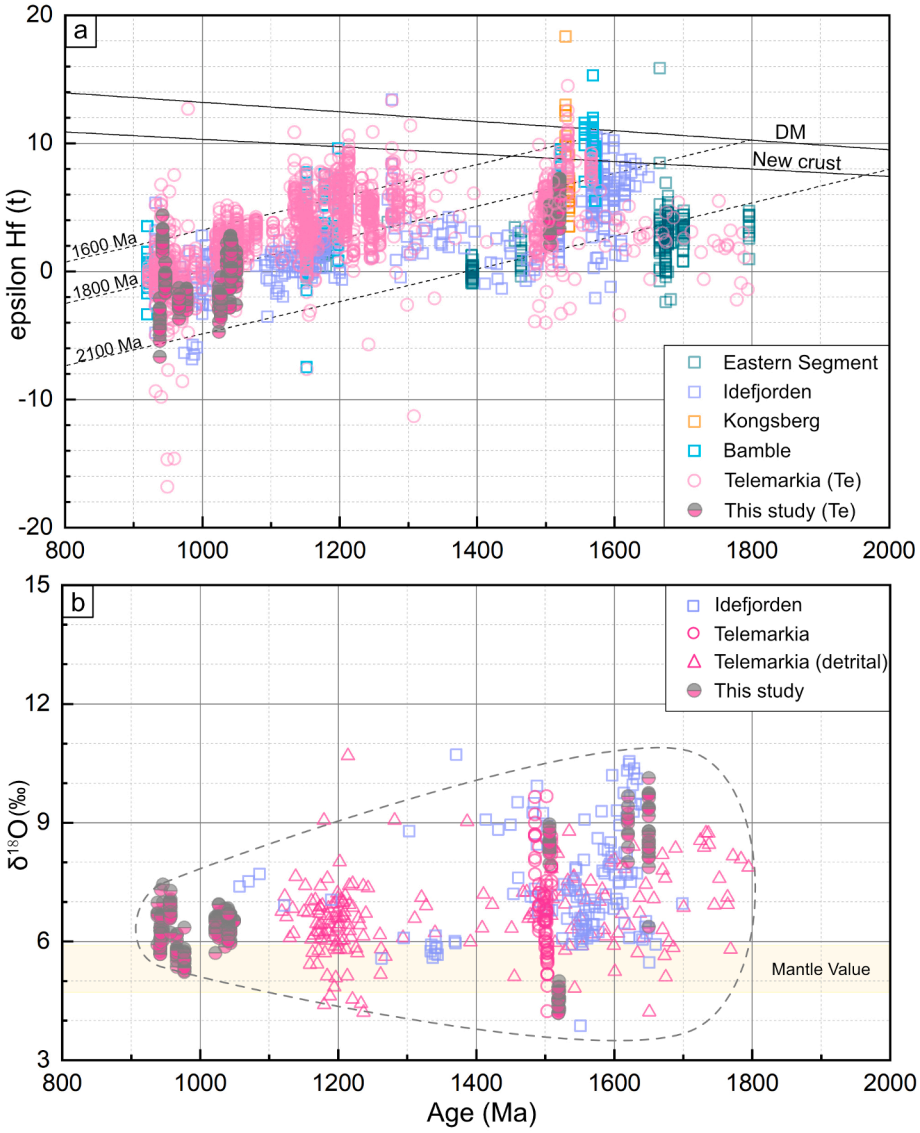

Fig. 8. Compiled Hf (a) and O (b) isotopic data in the Sveconorwegian Orogen (<1800 Ma). The Hf isotopic data of previous studies are from the data compilation in Granseth et al. (2021), Roberts and Slagstad (2015), Spencer et al. (2014) and Petersson et al. (2015). The O isotopic data are from Roberts et al. (2013), Spencer et al. (2014) and Petersson et al. (2015). The dash line field shows O isotopic variation; Gothian and Telemarkian crust has a wide range of $\delta^{18}O$ values while Sveconorwegian crust mostly shows moderate values.

crust-like Hf–O isotopic compositions with slightly negative to positive εHf(t) (−1–+3) and moderately elevated $\delta^{18}O$ values (6–6.5‰) (Fig. 7a), indicating a significant involvement of crustal components during magma genesis. Thus, they are not primary melts directly from the depleted mantle but most likely have a mixed origin of continental crust assimilated by mantle-derived magmas. Alternatively, the lithospheric mantle had probably been metasomatized (during early subduction) to have an enriched composition. Similar Hf and O isotopic signatures of ca. 1050 Ma mafic and granitic rocks is indicative of the possibility that granites could have formed by differentiation, through crystallization or melting, of coeval mafic material.

Previous studies interpreted that the magma sources of ca. 1050 Ma mafic and granitic rocks incorporated remelting of older continental crust and juvenile inputs, based on their geochemical and isotopic signatures (Bingen et al., 1993; Andersen et al., 2009; Granseth et al., 2021). Here, a mixing model between two endmembers of new crust ($\delta^{18}O = 5.7‰$, εHf(t) = +10.2) and 1.5 Ga Telemarkia crust ($\delta^{18}O = 7‰$, εHf(t) = − 4.5) has been used to estimate the potential contribution of juvenile additions and continental crust (Fig. 7b). The εHf(t) value of the older crust is in line with the Hf isotopic composition of ca. 1030 Ma leucogranite sample ØC-07 (average εHf(t) = − 4.2 ± 0.7), assuming it represents pure crustal melts, and the $\delta^{18}O$ value is consistent with the average lower continental crust. Overall, the modelling results show that ca. 1050 Ma rocks have an isotopic composition of 50% anatectic melts from older crust mixing with a similar proportion of juvenile magmas, which is broadly consistent with the modelling results based on trace element and radioisotope compositions in a recent study (Granseth et al., 2021). It should be noted however, that the contribution from the older crustal components is probably underestimated, as the ca. 1500 Ma Telemarkian crust as a whole has a wide range of isotopic values that cover the isotopic compositions of the Sveconorwegian rocks (Fig. 7b). Overall, the ca. 1050 Ma magmas were most likely derived from the remelting of crustal components with possible juvenile inputs, although it is problematic to precisely constarin the relative proportions of the crustal- and mantle-derived components. The ca. 1030 Ma leucogranites with more evolved Hf isotopic compositions may represent purer crustal melts that derived from a higher proportion of ca. 1.5 Ga Telemarkian crustal components.

In contrast to the N-S trending distribution of the SMB restricted to the Telemarkia unit, the HBG are sporadically exposed in the Telemarkia, Bamble and Idefjorden lithotectonic units. They range in composition from gabbronorite to granite (55–72 wt% SiO_2), which is interpreted to reflect extreme fractional crystallization of several batches of basaltic magma (Bogaerts et al., 2003). The HBG suite was interpreted to be derived from an undepleted to slightly depleted hydrous mafic source that was underplated during previous orogenic

events (Bogaerts et al., 2003; Vander Auwera et al., 2003). An alternative interpretation considered granitic magmas as products of mixing of crustal anatectic melts and mafic, mantle-derived magmas (Andersen et al., 2009). In addition, it has been recently proposed that rocks of the HBG suite outside and inside the SMB have different derivations, with the former derived by about 50% remelting of the ca. 1.5 Ga continental crust, while the latter derived from low-degree remelting of the residual continental crust after the extraction of the SMB granitic magmas (Granseth et al., 2020). All of these studies indicate that the source of the HBG (in the SMB) rocks has a complicated and heterogeneous composition, probably involving older and newly underplated mafic crust, residues of continental crust and mantle-derived juvenile magmas. The 980–930 Ma HBG granites in this study show a relatively wide range of Hf isotopic values from −4 to +3 (Fig. 7a), indicating various contributions from multiple mantle- and crust-derived components.

In summary, although the surface expression of ca. 1050 Ma mafic rocks is very limited, it would to some degree produce the parental magmas of the voluminous granitic rocks, and thus mafic underplating probably provided the source of both heating and material to generate granitic magmas. These granites were most likely derived from a mixed source of older Telemarkian and coeval mafic crust. The magma mixing processes could have happened in some sort of area for magma storage at the base of the continental crust, corresponding with the zone where melting, assimilation, storage and homogenization take place (MASH zone, Hildreth and Moorbath, 1988) or within a deep crustal hot zone (Annen et al., 2006). In such a zone, extensive mafic underplating caused remelting of lower crustal rocks, and the efficient magma hybridization resulted in ca. 1050 Ma granitic magmas with homogenous isotopic compositions.

6.3. *Tectonic implications: comparison with typical accretionary margins in Hf–O isotopic composition*

The 1050–930 Ma magmatism, which characterized the Sveconorwegian orogenic activities in southwest Norway, was interpreted to have happened under a post-collisional extensional environment associated with the delamination and foundering of the lithospheric mantle (e.g. Bingen et al., 2021). An alternative interpretation explained it as subduction-related magmatism that is comparable to arc magmatic activities in cordilleran systems (Coint et al., 2015), with a part of evidence from the arc-like whole-rock geochemistry and isotopic compositions (Slagstad et al., 2013; Granseth et al., 2020). However, as previous studies pointed out, the geochemical signatures of these granites were largely inherited from the pre-existing Telemarkian crust and this information alone appears to be unable to directly distinguish whether the granites formed in a subduction- or collision-related setting (e.g. Bingen et al., 2021).

Combined zircon Hf–O isotopic data of 1050–930 Ma Sveconorwegian magmas reported for the first time in this study provide an opportunity to compare their isotopic signatures with those of typical

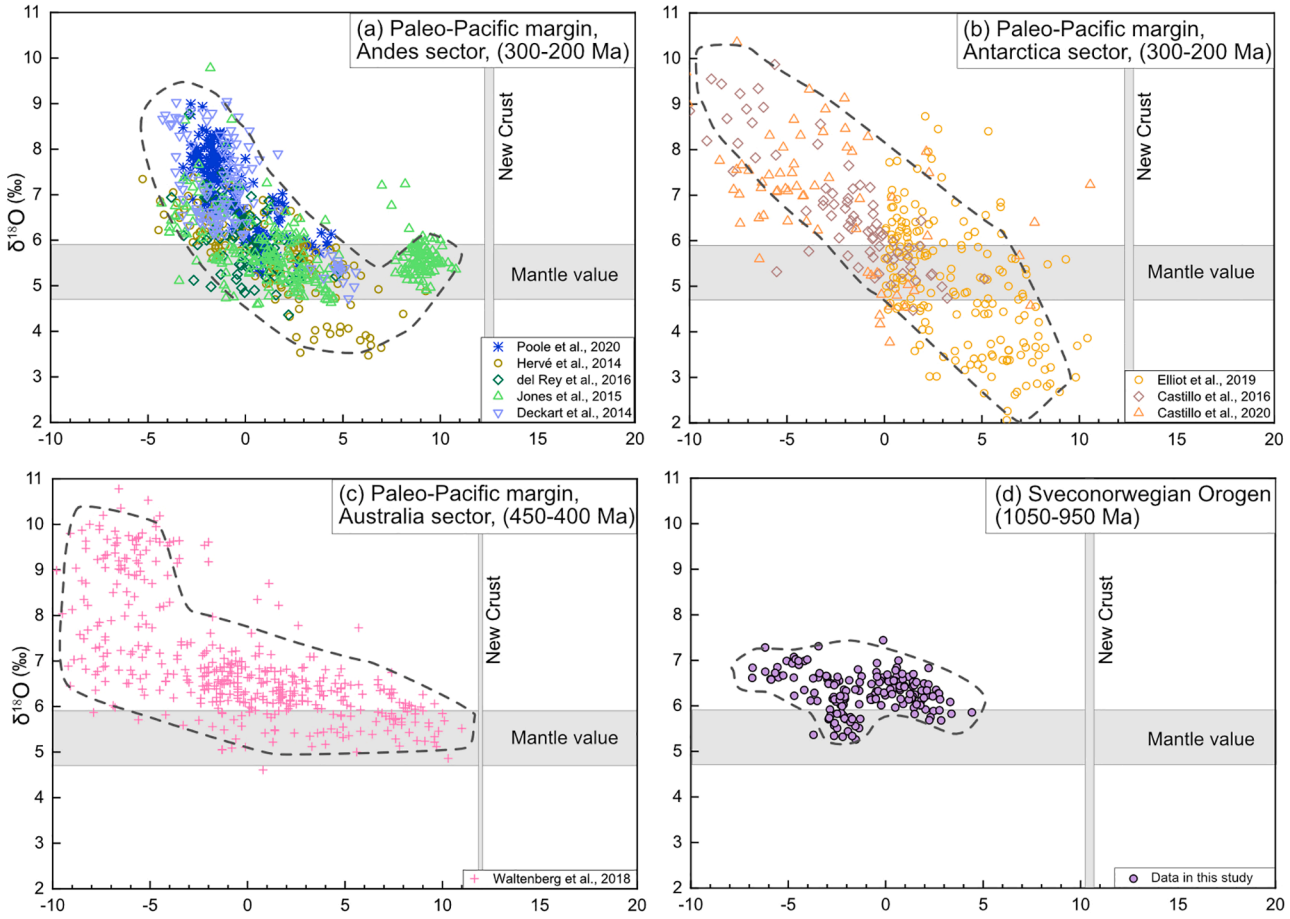

Fig. 9. Initial epsilon Hf values versus $\delta^{18}O$ values of magmatic and detrital zircons from the Paleo-Pacific margin (a-c) and the Sveconorwegian orogen (d). The Sveconorwegian magmas have distinct Hf–O isotopic patterns from the arc magmas along the Paleo-Pacific margin, but it is noted that the Australia sector is comparable to a West-Pacific type margin in contrast to Andean-style orogeny from South America to West Antarctica. The data of the Andes sector are from Deckart et al. (2014), Hervé et al., (2014), Jones et al. (2015), del Rey et al. (2016), Poole et al. (2020), those of Antarctica sector are from Castillo et al. (2016) and Castillo et al. (2020), Elliot et al. (2019) and those of Australia sector are from Waltenberg et al. (2018). Grey horizontal bars show O isotopic range of mantle-derived magmas, and vertical bars show εHf(t) range of the new crust (Dhuime et al., 2011) at the corresponding age.

accretionary orogens, e.g. those along the Paleo-Pacific margin. The Paleo-Pacific margin developed as a long-lived active continental margin on the southern periphery of Gondwana, forming a series of accretionary orogens along the coast of South America (Andes), West Antarctica and eastern Australia. We compiled the Hf–O isotopic data of magmatic and detrital zircons from the Andes in Argentina and Chile (ca. 300–200 Ma), the Antarctic Peninsula (ca. 300–200 Ma) and the Lachlan and Thomson orogens of the Australian sector (450–400 Ma) (Fig. 9a–c). Irrespective of the spatial and temporal variations of isotopic compositions, εHf(t) and $\delta^{18}O$ values from the three sectors consistently show a marked negative correlation. The common information obtained from their Hf–O isotopic patterns is that sedimentary components with evolved Hf and highly elevated O isotopic values and relatively juvenile magmas with radiogenic isotopes that are close to the values of the new crust have been largely incorporated in these arc magmas (Fig. 9a–c). A similar isotopic correlation has also been observed from the ca. 1500 Ma Telemarkian rocks, consistent with their formation in a subduction-related setting (Roberts et al., 2013). In contrast, ca. 1050–930 Ma Sveconorwegian magmas have relatively homogeneous, moderate $\delta^{18}O$ values, and thus their zircon Hf and O isotopic patterns distinguish them from typical arc magmas (Fig. 9d). Considering the limited sampling area in this study, we suggest that more combined Hf–O isotopic studies, especially on the samples from South Norway, are probably required (as one granite sample with high $\delta^{18}O$ values of 11–12‰ was reported by Roberts, 2010). However, the isotopic data reported here are consistent with the geological expressions, as the granitic rocks are mostly I- and A-type, while S-type granites are mostly lacking in the Sveconorwegian (Slagstad et al., 2013; Coint et al., 2015; Granseth et al., 2020).

Overall, presently available Hf–O isotopic data indicate that the 1050–930 Ma Sveconorwegian magmas show little isotopic fingerprint that are expected in an active subduction setting, as their formation witnessed significantly less input of sedimentary components and juvenile mantle-derived magmas than arc magmas generated in typical accretionary margins. From this perspective, the 1050–930 Ma Sveconorwegian magmas are not compatible with a continuous supra-subduction setting. Synchronous emplacement of mafic and granitic rocks (although mafic rocks usually have a limited exposure) is commonly observed in post-collisional settings, such as in the Variscan belt (Couzinié et al., 2016), the Caledonian orogeny in Scotland (Clemens et al., 2009), the East African-Antarctic Orogen (Wang et al., 2020), etc. The post-collisional mafic rocks generally have a relatively evolved isotopic compsotion, in contrast to mafic arc magmas that

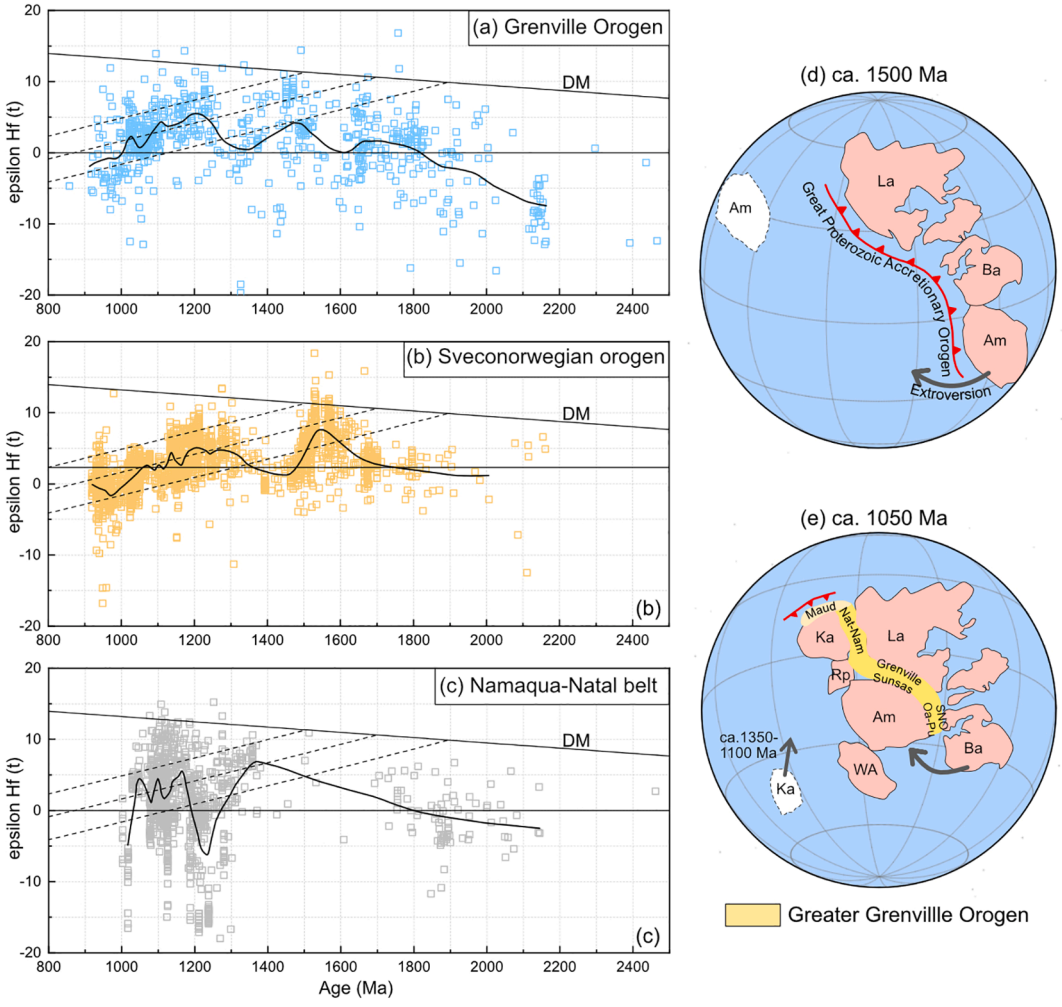

Fig. 10. (a–c) Hf isotopic evolution of the Grenville Orogen (a, data from Spencer et al., 2019), of the Sveconorwegian orogen (b, data are the same as Fig. 9), of the Namaqua-Natal belt (c, data from Spencer et al., 2015; Hall et al., 2018; Martin et al., 2020). The black lines show LOWESS smoothing results; (d) Paleogeographic reconstruction at ca. 1500 Ma (modified after Johansson, 2009; Evans and Mitchell, 2011) with the margins of Laurentia, Baltica and Amazonia as a greater Proterozoic accretionary margin (Condie, 2013). An alternative position of Amazonia that was unconnected with Laurentia-Baltica is also shown (Pisarevsky et al., 2014); (e) Paleogeographic reconstruction at ca. 1050 Ma, showing a possibly continuous Grenville Orogen (after Li et al., 2008, Cawood and Pisarevsky, 2017). Am, Amazonia; Ba, Baltica; Ka, Kalahari; La, Laurentia; Nat-Nam, Natal-Namaqua belt; Oa, Oaxaquia; Pu, Putumayo orogen; RP, Río de la Plata; SNO, Sveconorwegian orogen; WA, West Africa.

usually show juvenile isotopic signatures.

6.4. Mesoproterozoic accretionary and collisional orogenesis in the core of Rodinia

In various paleogeographic reconstructions, Laurentia, Amazonia, Baltica and Kalahari constitute the core of the supercontinent Rodinia, where well-preserved remnants of Grenville-age orogenic belts provide a key to understanding their configuration and interactions during Mesoproterozoic times (Li et al., 2008; Merdith et al., 2017; Martin et al., 2020). These Grenville-age belts were largely established on a long-lived accretionary system (ca. 1800–1300 Ma) that developed along the margin of the supercontinent Columbia/Nuna (Columbia hereafter) from Laurentia to Amazonia (Fig. 10d, but see Pisarevsky et al., 2014, who placed Amazonia in a distant position from Laurentia and Baltica), which is associated with the subduction of an exterior ocean to Columbia (Condie, 2013; Roberts, 2013). During the transition from Columbia to Rodinia, the evolution of these three continents appeared to be characterized by the closure of the exterior ocean, and this accretionary margin subsequently turned 'outside in', finally leading to Grenville-age continental collision (e.g. Evans, 2013; Martin et al., 2020). In Laurentia and Baltica, the Hf isotopic compositions of Grenville-age rocks reflect an important contribution of pre-existing crustal components (Fig. 10a, b), typical for continent–continent collisional orogenic systems, where an increasing amount of evolved material is incorporated into melts over time due to crustal thickening (e.g. Spencer et al., 2019).

Following Mesoproterozoic accretionary orogeny, it has been well constrained by paleomagnetic data that Baltica had rotated >90° clockwise by ca. 990 Ma with its western margin (present-day coordinates and the same thereafter) broadly facing the margin of Laurentia-Greenland (Cawood and Pisarevsky, 2017), but the position of Baltica relative to Laurentia and Amazonia is still debated with various models proposed (see reviews in Bingen et al., 2021). The classical collisional model places the Sveconorwegian orogen facing the northern margin of Amazonia and considers the orogen as the product of continental collision between Baltica and Amazonia with the Putumayo orogen and Oaxaquia in between (Park, 1992; Karlstrom et al., 2001; Bogdanova et al., 2008; Weber et al., 2010; Ibanez-Mejia et al., 2011; Cawood and Pisarevsky, 2017; Ibañez-Mejia, 2020). An alternative view correlates the Sveconorwegian orogen as the opposing collisional margin of the northern Grenville Province in Labrador, mainly based on their comparable ca. 1050 Ma and ca. 950 Ma granitic rocks (Johansson, 2009, 2014). Alternatively, an accretionary model placed Baltica at a position that is relatively distant from Laurentia and Amazonia, and interpreted Sveconorwegian Baltica as a long-term accretionary margin (e.g., Slagstad et al., 2017, 2020). In addition, another model interprets the four western Sveconorwegian lithotectonic units as one plate (exotic to Baltica) that collided with the Eastern Segment (endemic to Baltica) at ca. 990 Ma (Möller and Andersson, 2018). Testing these models is not the aim of this paper. However, as discussed above, the very minor to neglectable involvement of sedimentary components during the formation of ca. 1050–930 Ma Sveconorwegian rocks compared with other typical arc magmas appears to be incompatible with a purely subduction-accretion processes during this time interval.

The position of Kalahari in supercontinent Columbia has been poorly constrained due to a lack of well-defined paleomagnetic data, and it was either not considered as a part of Columbia or was placed along the distant periphery of the supercontinent (e.g. Pesonen et al., 2012; Pisarevsky et al., 2014). However, paleomagnetic data show that from Columbia break-up to Rodinia assembly, Kalahari travelled northwards from a high latitude at ca. 1350 Ma until arriving at an equatorial position at ca. 1110 Ma (Fig. 10e, de Kock et al., 2019). Thus, in contrast to Laurentia, Baltica and Amazonia with a long-term juxtaposition from Columbia to Rodinia, Kalahari appeared as an exotic continental block that was incorporated into this 'family' during the amalgamation of Rodinia. During ca. 1350–1110 Ma, the Kalahari margin along the Namaqua-Natal side witnessed multiple periods of arc/back-arc magmatic activities and accretion of oceanic arcs, with both juvenile and rather evolved Hf isotopic signatures indicating a variable contribution of older crustal components (Fig. 10c). Kalahari collided with Laurentia along the Namaqua-Natal margin after rapid southward drift of Laurentia at ca. 1110–1080 Ma (Loewy et al., 2011; Swanson-Hysell et al., 2015, 2019).

It is suggested that core constituents of Rodinia including Laurentia, Amazonia, Baltica and Kalahari were connected by a continuous Grenville-age orogenic belt (Fig. 10e), which probably developed at ca. 1050 Ma. As the archetypal example of the Grenville-age orogens, the Grenville Orogen was constructed as a product of prolonged collision between Amazonia and Laurentia during ca. 1080–980 Ma (Hynes and Rivers, 2010). It probably extended westward through the collision between Kalahari and Laurentia. On its eastern side, the Sveconorwegian Orogen represents the extension of the Grenville Orogen into southwest Baltica, and the orogen most likely formed by collisional interactions of Baltica with Amazonia and/or Laurentia.

7. Summary and conclusions

Crust with a Sveconorwegian magmatic and metamorphic overprint is described in the Baltican basement of the Caledonides, including the Hardangerfjord area, the Øygarden Complex and the Western Gneiss Region (Gulen and Nordfjord areas). New combined U–Pb, Lu–Hf and O isotopic data show that the crust in the Baltican basement of the southern Scandinavian Caledonides correlates well with the crust exposed in the western Sveconorwegian orogen in South Norway, as they have similar geochronological and isotopic characteristics.

1. In the Hardangerfjord area, the crust has a Telemarkian affinity, which was generated at ca. 1520–1480 Ma, probably in a juvenile magmatic arc setting (Suldal volcanic arc). At the northern end of the studied area, the Nordfjord area of the Western Gneiss Region, the crust has Gothian protolith ages, with orthogneiss dated at ca. 1650–1620 Ma and less juvenile isotopic signatures. In between these two areas, within the Øygarden Complex and Gulen dome, the protolith ages are transitional with evidence for both Gothian and Telemarkian ages.
2. Sveconorwegian magmatism includes two main magmatic suites. The ca. 1050–1020 Ma magmatism in the Hardangerfjord area and the Øygarden Complex attests to the northward continuation of the Sirdal Magmatic Belt. Our new data demonstrate that the Sirdal Magmatic Belt is much more extensive than previously thought. It extends for at least 300 km in West Norway, geographically overlapping with the Telemarkian Suldal volcanic arc. The ca. 980–930 Ma granite plutons are found in the Hardangerfjord area and the Western Gneiss Region (Gulen and Nordfjord areas), and are correlated with the hornblende–biotite granite suite exposed in the rest of the Sveconorwegian orogen.
3. The Øygarden Complex and the Gulen dome in the southern Western Gneiss Region experienced high-grade metamorphism and migmatization during the Sveconorwegian orogenesis, which occurred predominantly during 1060 and 1020 Ma with a peak at ca. 1030 Ma. It is temporally and spatially related to the formation and emplacement of the Sirdal Magmatic Belt.
4. The northern limit of ca. 1050 Ma magmatic and metamorphic events of the Øygarden Complex and the Gulen area corresponds to the boundary between Telemarkian and Gothian crust, and these crustal heterogeneities probably controlled the development of Caledonian shear zones.
5. Zircon Hf–O isotopic patterns indicate relatively less involvement of supracrustal (sedimentary) and juvenile material during the formation of ca.1050–930 Ma Sveconorwegian magmas in comparison to typical arc magmas, which makes the southwestern margin of Baltica

appear to be incompatible with a long-term subduction setting during Rodinia assembly.

Collectively, the new data show that the Precambrian crustal architecture and isotopic signatures in the study area are largely coherent with the Sveconorwegian Province that was unaffected by the Caledonian orogeny. A continental collisional setting is favored to interpret the orogenic history of the Sveconorwegian orogen, but specific tectonic models and the configuration of Baltica in relation to Laurentia and Amazonia remain open questions in the context of Rodinia reconstructions.

CRediT authorship contribution statement

Cheng-Cheng Wang: Conceptualization, Formal analysis, Investigation, Resources, Writing - original draft, Writing - review & editing, Visualization, Funding acquisition. **Johannes D. Wiest:** Investigation, Formal analysis, Resources, Writing - original draft, Visualization, Writing - review & editing. **Joachim Jacobs:** Investigation, Supervision, Project administration, Writing - review & editing. **Bernard Bingen:** Investigation, Writing - review & editing, Supervision. **Martin J. Whitehouse:** Validation, Data curation, Formal analysis. **Marlina A. Elburg:** Validation, Data curation, Formal analysis, Writing - review & editing. **Thea S. Sørstrand:** Resources. **Lise Mikkelsen:** Resources. **Åse Hestnes:** Resources.

Declaration of Competing Interest

The authors declare that they have no known competing financial interests or personal relationships that could have appeared to influence the work reported in this paper.

Acknowledgements

This study is a part of the PhD project of the first author. It was financially supported by faculty-specific funds and endowments of the Faculty of Mathematics and Natural Sciences, University of Bergen (NO. 814220), and the Research Council of Norway through the funding to The Norwegian Research School on Dynamics and Evolution of Earth and Planets (NO. 249040/F60). C-C. Wang is grateful to the support from the China Scholarship Council. We furthermore acknowledge funding from VISTA – a basic research collaboration between the Norwegian Academy of Science and Letters and Equinor (grants no. 6271, 6274). The MC-ICP-MS lab at UJ was funded by NRF-NEP grant 93208, and is supported by DSI-NRF CIMERA. M. A. Elburg acknowledges NRF IFRR funding (No. 119297). Deta Gasser is thanked for help with some of the sampling in the Western Gneiss Region. We thank Nick M.W. Roberts and an anonymous referee for their constructive comments and suggestions, which greatly helped to improve the manuscript. This is NordSIM publication #686.

Appendix A. Supplementary data

Supplementary data to this article can be found online at https://doi.org/10.1016/j.precamres.2021.106301.

References

Åhäll, K.I., Larson, S.Å., 2000. Growth-related 1.85–1.55 Ga magmatism in the Baltic Shield; a review addressing the tectonic characteristics of Svecofennian, TIB 1-related, and Gothian events. Geol. Foeren. Stockholm Foerh. 122, 193–206.
Andersen, T.B., Osmundsen, P.T., Jolivet, L., 1994. Deep crustal fabrics and a model for the extensional collapse of the southwest Norwegian Caledonides. J. Struct. Geol. 16, 1191–1203.
Andersen, T., Andresen, A., Sylvester, A.G., 2001. Nature and distribution of deep crustal reservoirs in the southwestern part of the Baltic Shield: evidence from Nd, Sr and Pb isotope data on late Sveconorwegian granites. J. Geol. Soc. 158, 253–267.
Andersen, T., Griffin, W.L., Pearson, N.J., 2002. Crustal evolution in the SW part of the Baltic Shield: the Hf isotope evidence. J. Petrol. 43, 1725–1747.
Andersen, T., Griffin, W.L., Sylvester, A.G., 2007. Sveconorwegian crustal underplating in southwestern Fennoscandia: LAM-ICPMS U-Pb and Lu–Hf isotope evidence from granites and gneisses in Telemark, southern Norway. Lithos 93, 273–287.
Andersen, T., Graham, S., Sylvester, A.G., 2009. The geochemistry, Lu–Hf isotope systematics, and petrogenesis of Late Mesoproterozoic A-type granites in southwestern Fennoscandia. Can. Mineral. 47, 1399–1422.
Annen, C., Blundy, J.D., Sparks, R.S.J., 2006. The genesis of intermediate and silicic magmas in deep crustal hot zones. J. Petrol. 47, 505–539.
Ashwal, L.D., 1993. In: Anorthosites. Springer-Verlag, Berlin, p. 422.
Austrheim, H., Corfu, F., Bryhni, I., Andersen, T.B., 2003. The Proterozoic Hustad igneous complex: a low strain enclave with a key to the history of the Western Gneiss Region of Norway. Precambr. Res. 120, 149–175.
Beckman, V., Möller, C., Söderlund, U., Corfu, F., Pallon, J., Chamberlain, K.R., 2014. Metamorphic zircon formation at the transition from gabbro to eclogite in Trollheimen-Surnadalen, Norwegian Caledonides. In: Geological Society, London, Special Publication, pp. 403–424.
Bergström, U., Stephens, M.B., Wahlgren, C.H., 2020. Polyphase (1.6–1.5 and 1.1–1.0 Ga) deformation and metamorphism of Proterozoic (1.7–1.1 Ga) continental crust, Idefjorden terrane, Sveconorwegian orogen. In: Geological Society, London, Memoirs, pp. 397–434.
Bingen, B., Demaiffe, D., Hertogen, J., Weis, D., Michot, J., 1993. K-rich calc-alkaline augen gneisses of Grenvillian age in SW Norway: mingling of mantle-derived and crustal components. J. Geol. 101, 763–778.
Bingen, B., Demaiffe, D., Breemen, O.V., 1998. The 616 Ma old Egersund basaltic dike swarm, SW Norway, and late Neoproterozoic opening of the Iapetus Ocean. J. Geol. 106, 565–574.
Bingen, B., Skår, Ø., Marker, M., Sigmond, E.M., Nordgulen, Ø., Ragnhildstveit, J., Mansfeld, J., Tucker, R.D., Liégeois, J.P., 2005. Timing of continental building in the Sveconorwegian orogen, SW Scandinavia. Norw. J. Geol. /Norsk Geologisk Forening 85.
Bingen, B., Stein, H.J., Bogaerts, M., Bolle, O., Mansfeld, J., 2006. Molybdenite Re–Os dating constrains gravitational collapse of the Sveconorwegian orogen, SW Scandinavia. Lithos 87, 328–346.
Bingen, B., Nordgulen, Ø., Viola, G., 2008a. A four-phase model for the Sveconorwegian orogeny, SW Scandinavia. Norw. J. Geol. /Norsk Geologisk Forening 88 (1).
Bingen, B., Davis, W.J., Hamilton, M.A., Engvik, A.K., Stein, H.J., Skår, Ø., Nordgulen, Ø., 2008b. Geochronology of high-grade metamorphism in the Sveconorwegian belt, S. Norway: U-Pb, Th-Pb and Re-Os data. Norw. J. Geol. /Norsk Geologisk Forening 88 (1).
Bingen, B., Andersson, J., Soderlun, U., Moller, C., 2008c. The Mesoproterozoic in the Nordic countries. Episodes 31, 29.
Bingen, B., Corfu, F., Stein, H.J., Whitehouse, M.J., 2015. U-Pb geochronology of the syn-orogenic Knaben molybdenum deposits, Sveconorwegian orogen, Norway. Geol. Mag. 152, 537–556.
Bingen, B., Viola, G., 2018. The early-Sveconorwegian orogeny in southern Norway: Tectonic model involving delamination of the sub-continental lithospheric mantle. Precambr. Res. 313, 170–204.
Bingen, B., Viola, G., Möller, C., Vander Auwera, J., Laurent, A., Yi, K., 2021. The Sveconorwegian orogeny. Gondwana Res. 90, 273–313.
Blereau, E., Johnson, T.E., Clark, C., Taylor, R.J., Kinny, P.D., Hand, M., 2017. Reappraising the P-T evolution of the rogaland–vest agder sector, southwestern Norway. Geosci. Front. 8, 1–14.
Bogaerts, M., Scaillet, B., Liégeois, J.P., Vander Auwera, J., 2003. Petrology and geochemistry of the Lyngdal granodiorite (Southern Norway) and the role of fractional crystallisation in the genesis of Proterozoic ferro-potassic A-type granites. Precambrian Research 124, 149–184.
Bogdanova, S.V., Bingen, B., Gorbatschev, R., Kheraskova, T.N., Kozlov, V.I., Puchkov, V. N., Volozh, Y.A., 2008. The East European Craton (Baltica) before and during the assembly of Rodinia. Precambr. Res. 160, 23–45.
Bogdanova, S., Gorbatschev, R., Skridlaite, G., Soesoo, A., Taran, L., Kurlovich, D., 2015. Trans-Baltic Palaeoproterozoic correlations towards the reconstruction of supercontinent Columbia/Nuna. Precambr. Res. 259, 5–33.
Bouvier, A., Vervoort, J.D., Patchett, P.J., 2008. The Lu–Hf and Sm–Nd isotopic composition of CHUR: constraints from unequilibrated chondrites and implications for the bulk composition of terrestrial planets. Earth and Planetary Science Letters 273, 48–57.
Brueckner, H.K., 2018. The great eclogite debate of the Western Gneiss Region, Norwegian Caledonides: the in situ crustal v. exotic mantle origin controversy. J. Metamorph. Geol. 36, 517–527.
Bybee, G.M., Ashwal, L.D., Shirey, S.B., Horan, M., Mock, T., Andersen, T.B., 2014. Pyroxene megacrysts in Proterozoic anorthosites: Implications for tectonic setting, magma source and magmatic processes at the Moho. Earth and Planetary Science Letters 389, 74–85.
Castillo, P., Fanning, C.M., Hervé, F., Lacassie, J.P., 2016. Characterisation and tracing of Permian magmatism in the south-western segment of the Gondwanan margin; U-Pb age, Lu–Hf and O isotopic compositions of detrital zircons from metasedimentary complexes of northern Antarctic Peninsula and western Patagonia. Gondwana Res. 36, 1–13.
Castillo, P., Fanning, C.M., Riley, T.R., 2020. Zircon O and Hf isotopic constraints on the genesis of Permian-Triassic magmatic and metamorphic rocks in the Antarctic Peninsula and correlations with Patagonia. J. S. Am. Earth Sci. 104, 102848.
Cawood, P.A., McCausland, P.J., Dunning, G.R., 2001. Opening Iapetus: constraints from the Laurentian margin in Newfoundland. Geol. Soc. Am. Bull. 113, 443–453.

Cawood, P.A., Pisarevsky, S.A., 2017. Laurentia-Baltica-Amazonia relations during Rodinia assembly. Precambr. Res. 292, 386–397.
Clemens, J.D., Darbyshire, D.P.F., Flinders, J., 2009. Sources of post-orogenic calcalkaline magmas: the Arrochar and Garabal Hill-Glen Fyne complexes, Scotland. Lithos 112, 524–542.
Cocks, L.R.M., Torsvik, T.H., 2005. Baltica from the late Precambrian to mid-Palaeozoic times: the gain and loss of a terrane's identity. Earth Sci. Rev. 72, 39–66.
Coint, N., Slagstad, T., Roberts, N.M.W., Marker, M., Røhr, T., Sørensen, B.E., 2015. The Late Mesoproterozoic Sirdal Magmatic Belt, SW Norway: relationships between magmatism and metamorphism and implications for Sveconorwegian orogenesis. Precambr. Res. 265, 57–77.
Condie, K.C., 2013. Preservation and recycling of crust during accretionary and collisional phases of Proterozoic orogens: A bumpy road from Nuna to Rodinia. Geosciences 3, 240–261.
Corfu, F., Andersen, T.B., Gasser, D., 2014a. The Scandinavian Caledonides: main features, conceptual advances and critical questions. In: Geological Society, London, Special Publication, pp. 9–43.
Corfu, F., Austrheim, H., Ganzhorn, A.C., 2014b. Localized granulite and eclogite facies metamorphism at Flatraket and Kråkeneset, Western Gneiss Region: U-Pb data and tectonic implications. In: Geological Society, London, Special Publication, pp. 425–442.
Cosca, M.A., Mezger, K., Essene, E.J., 1998. The Baltica-Laurentia connection: Sveconorwegian (Grenvillian) metamorphism, cooling, and unroofing in the Bamble sector, Norway. J. Geol. 106, 539–552.
Couzinié, S., Laurent, O., Moyen, J.F., Zeh, A., Bouilhol, P., Villaros, A., 2016. Post-collisional magmatism: crustal growth not identified by zircon Hf–O isotopes. Earth Planet. Sci. Lett. 456, 182–195.
Dalziel, I.W., 1997. OVERVIEW: Neoproterozoic-Paleozoic geography and tectonics: review, hypothesis, environmental speculation. Geol. Soc. Am. Bull. 109, 16–42.
Dalziel, I.W., Mosher, S., Gahagan, L.M., 2000. Laurentia-Kalahari collision and the assembly of Rodinia. J. Geol. 108, 499–513.
Deckart, K., Hervé Allamand, F., Fanning, M., Ramírez, V., Calderón, M., Godoy, E., 2014. U-Pb geochronology and Hf-O isotopes of zircons from the Pennsylvanian Coastal Batholith, south-central Chile. Andean Geol. 41, 49–82.
de Kock, M.O., Gumsley, A.P., Klausen, M.B., Söderlund, U., Djeutchou, C., 2019. The Precambrian mafic magmatic record, including large igneous provinces of the Kalahari craton and its constituents: A paleogeographic review. Dyke Swarms of the World: A Modern Perspective, pp. 155–214.
del Rey, A., Deckart, K., Arriagada, C., Martínez, F., 2016. Resolving the paradigm of the late Paleozoic-Triassic Chilean magmatism: isotopic approach. Gondwana Res. 37, 172–181.
Dhuime, B., Hawkesworth, C., Cawood, P., 2011. When continents formed. Science 331, 154–155.
Drüppel, K., Elsäßer, L., Brandt, S., Gerdes, A., 2013. Sveconorwegian mid-crustal ultrahigh-temperature metamorphism in Rogaland, Norway: U-Pb LA-ICP-MS geochronology and pseudosections of sapphirine granulites and associated paragneisses. J. Petrol. 54, 305–350.
Elliot, D.H., Fanning, C.M., Mukasa, S.B., Millar, I.L., 2019. Hf-and O-isotope data from detrital and granitoid zircons reveal characteristics of the Permian-Triassic magmatic belt along the Antarctic sector of Gondwana. Geosphere 15, 576–604.
Engvik, A.K., Austrheim, H., Andersen, T.B., 2000. Structural, mineralogical and petrophysical effects on deep crustal rocks of fluid-limited polymetamorphism, Western Gneiss Region, Norway. J. Geol. Soc. 157, 121–134.
Engvik, A.K., Bingen, B., Solli, A., 2016. Localized occurrences of granulite: P-T modeling, U–Pb geochronology and distribution of early-Sveconorwegian high-grade metamorphism in Bamble, South Norway. Lithos 240, 84–103.
Evans, D.A., Mitchell, R.N., 2011. Assembly and breakup of the core of Paleoproterozoic-Mesoproterozoic supercontinent Nuna. Geology 39, 443–446.
Evans, D.A., 2013. Reconstructing pre-Pangean supercontinents. Bulletin 125, 1735–1751.
Fossen, H., 1992. The role of extensional tectonics in the caledonides of South Norway. J. Struct. Geol. 14, 1033–1046.
Fossen, H., Hurich, C.A., 2005. The Hardangerfjord Shear Zone in SW Norway and the North Sea: a large-scale low-angle shear zone in the Caledonian crust. J. Geol. Soc. 162, 675–687.
Fossen, H., 2010. Extensional tectonics in the North Atlantic Caledonides: a regional view. In: Geological Society, London, Special Publication, pp. 767–793.
Fossen, H., Gabrielsen, R.H., Faleide, J.I., Hurich, C.A., 2014. Crustal stretching in the Scandinavian Caledonides as revealed by deep seismic data. Geology 42, 791–794.
Fossen, H., Khani, H.F., Faleide, J.I., Ksienzyk, A.K., Dunlap, W.J., 2016. Post-Caledonian extension in the West Norway–northern North Sea region: the role of structural inheritance. In: Geological Society, London, Special Publication, pp. 465–486.
Gee, D.G., Andréasson, P.G., Lorenz, H., Frei, D., Majka, J., 2015. Detrital zircon signatures of the Baltoscandian margin along the Arctic Circle Caledonides in Sweden: The Sveconorwegian connection. Precambr. Res. 265, 40–56.
Glodny, J., Kühn, A., Austrheim, H., 2008. Diffusion versus recrystallization processes in Rb–Sr geochronology: isotopic relics in eclogite facies rocks, Western Gneiss Region, Norway. Geochim. Cosmochim. Acta 72, 506–525.
Gorbatschev, R., Bogdanova, S., 1993. Frontiers in the Baltic shield. Precambr. Res. 64, 3–21.
Gordon, S.M., Whitney, D.L., Teyssier, C., Fossen, H., 2013. U-Pb dates and trace-element geochemistry of zircon from migmatite, Western Gneiss Region, Norway: significance for history of partial melting in continental subduction. Lithos 170, 35–53.
Gordon, S.M., Whitney, D.L., Teyssier, C., Fossen, H., Kylander-Clark, A., 2016. Geochronology and geochemistry of zircon from the northern Western Gneiss Region: Insights into the Caledonian tectonic history of western Norway. Lithos 246–247, 134–148.
Griffin, W.L., Pearson, N.J., Belousova, E., Jackson, S.E., van Achterbergh, E., O'Reilly, S. Y., Shee, S.R., 2000. The Hf isotope composition of cratonic mantle: LAM-MCICPMS analysis of zircon megacrysts in kimberlites. Geochim. Cosmochim. Acta 64, 133–147.
Granseth, A., Slagstad, T., Coint, N., Roberts, N.M., Røhr, T.S., Sørensen, B.E., 2020. Tectonomagmatic evolution of the Sveconorwegian orogen recorded in the chemical and isotopic compositions of 1070–920 Ma granitoids. Precambr. Res. 340, 105527.
Granseth, A., Slagstad, T., Roberts, N.M., Hagen-Peter, G., Kirkland, C.L., Møkkelgjerd, S. H., Røhr, T.S., Coint, N., Sørensen, B.E., 2021. Multi-isotope tracing of the 1.3–0.9 Ga evolution of Fennoscandia; crustal growth during the Sveconorwegian orogeny. Gondwana Res. 91, 31–39.
Hacker, B.R., Andersen, T.B., Johnston, S., Kylander-Clark, A.R., Peterman, E.M., Walsh, E.O., Young, D., 2010. High-temperature deformation during continental-margin subduction & exhumation: the ultrahigh-pressure Western Gneiss Region of Norway. Tectonophysics 480, 149–171.
Hall, W.S., Hitzman, M.W., Kuiper, Y.D., Kylander-Clark, A.R., Holm-Denoma, C.S., Moscati, R.J., Plink-Björklund, P., Enders, M.S., 2018. Igneous and detrital zircon U-Pb and Lu-Hf geochronology of the late Meso-to Neoproterozoic northwest Botswana rift: Maximum depositional age and provenance of the Ghanzi Group, Kalahari Copperbelt, Botswana and Namibia. Precambr. Res. 318, 133–155.
Hervé, F., Fanning, C.M., Calderón, M., Mpodozis, C., 2014. Early Permian to Late Triassic batholiths of the Chilean Frontal Cordillera (28°-31°S): SHRIMP U-Pb zircon ages and Lu-Hf and O isotope systematics. Lithos 184–187, 436–446.
Hildreth, W., Moorbath, S., 1988. Crustal contributions to arc magmatism in the Andes of central Chile. Contrib. Miner. Petrol. 98, 455–489.
Hoffman, P.F., 1991. Did the breakout of Laurentia turn Gondwanaland inside-out? Science 252, 1409–1412.
Hynes, A., Rivers, T., 2010. Protracted continental collision—evidence from the Grenville orogen. Can. J. Earth Sci. 47, 591–620.
Ibanez-Mejia, M., Ruiz, J., Valencia, V.A., Cardona, A., Gehrels, G.E., Mora, A.R., 2011. The Putumayo Orogen of Amazonia and its implications for Rodinia reconstructions: New U-Pb geochronological insights into the Proterozoic tectonic evolution of northwestern South America. Precambr. Res. 191, 58–77.
Ibañez-Mejia, M., 2020. The Putumayo Orogen of Amazonia: A synthesis. In: Gómez, J., Mateus–Zabala, D. (eds.), The Geology of Colombia, Volume 1 Proterozoic–Paleozoic. Servicio Geológico Colombiano, Publicaciones Geológicas Especiales 35, 101–131. Bogotá.
Jacobs, J., Pisarevsky, S., Thomas, R.J., Becker, T., 2008. The Kalahari Craton during the assembly and dispersal of Rodinia. Precambrian Research 160, 142–158.
Jakob, J., Andersen, T.B., Kjøll, H.J., 2019. A review and reinterpretation of the architecture of the South and South-Central Scandinavian Caledonides—a magma-poor to magma-rich transition and the significance of the reactivation of rift inherited structures. Earth Sci. Rev. 192, 513–528.
Johansson, Å., 2009. Baltica, Amazonia and the SAMBA connection—1000 million years of neighbourhood during the Proterozoic? Precambr. Res. 175, 221–234.
Johansson, Å., 2014. From Rodinia to Gondwana with the 'SAMBA' model—a distant view from Baltica towards Amazonia and beyond. Precambr. Res. 244, 226–235.
Jones, R.E., Kirstein, L.A., Kasemann, S.A., Dhuime, B., Elliott, T., Litvak, V.D., Alonso, R., Hinton, R., Facility, E.I.M., 2015. Geodynamic controls on the contamination of Cenozoic arc magmas in the southern Central Andes: insights from the O and Hf isotopic composition of zircon. Geochim. Cosmochim. Acta 164, 386–402.
Karlstrom, K.E., Åhäll, K.I., Harlan, S.S., Williams, M.L., McLelland, J., Geissman, J.W., 2001. Long-lived (1.8–1.0 Ga) convergent orogen in southern Laurentia, its extensions to Australia and Baltica, and implications for refining Rodinia. Precambr. Res. 111, 5–30.
Krabbendam, M., Wain, A., Andersen, T.B., 2000. Pre-Caledonian granulite and gabbro enclaves in the Western Gneiss Region, Norway: indications of incomplete transition at high pressure. Geol. Mag. 137, 235–255.
Krogh, T.E., Kamo, S.L., Robinson, P., Terry, M.P., Kwok, K., 2011. U-Pb zircon geochronology of eclogites from the Scandian Orogen, northern Western Gneiss Region, Norway: 14–20 million years between eclogite crystallization and return to amphibolite-facies conditions. Can. J. Earth Sci. 48, 441–472.
Ksienzyk, A.K., Wemmer, K., Jacobs, J., Fossen, H., Schomberg, A.C., Sussenberger, A., Lunsdorf, N.K., Bastesen, E., 2016. Post-Caledonian brittle deformation in the Bergen area, West Norway: results from K-Ar illite fault gouge dating. Norw. J. Geol. 96, 275–299.
Kylander-Clark, A.R.C., Hacker, B.R., 2014. Age and significance of felsic dikes from the UHP western gneiss region. Tectonics 33, 2342–2360.
Labrousse, L., Jolivet, L., Agard, P., Hebert, R., Andersen, T.B., 2002. Crustal-scale boudinage and migmatization of gneiss during their exhumation in the UHP Province of Western Norway. Terra Nova 14, 263–270.
Labrousse, L., Jolivet, L., Andersen, T., Agard, P., Hébert, R., Maluski, H., Schärer, U., 2004. Pressure-temperature-time deformation history of the exhumation of ultra-high pressure rocks in the Western Gneiss Region, Norway. In: Geological Society of America Special Papers, pp. 155–183.
Laurent, A.T., Duchene, S., Bingen, B., Bosse, V., Seydoux-Guillaume, A.M., 2018a. Two successive phases of ultrahigh temperature metamorphism in Rogaland, S. Norway: evidence from Y-in-monazite thermometry. J. Metamorph. Geol. 36, 1009–1037.
Laurent, A.T., Bingen, B., Duchene, S., Whitehouse, M.J., Seydoux-Guillaume, A.M., Bosse, V., 2018b. Decoding a protracted zircon geochronological record in ultrahigh temperature granulite, and persistence of partial melting in the crust, Rogaland, Norway. Contrib. Mineral. Petrol. 173, 29.

Li, Z.X., Bogdanova, S.V., Collins, A.S., Davidson, A., De Waele, B., Ernst, R.E., Fitzsimons, I.C.W., Fuck, R.A., Gladkochub, D.P., Jacobs, J., Karlstrom, K.E., Lu, S., Natapov, L.M., Pease, V., Pisarevsky, S.A., Thrane, K., Vernikovsky, V., 2008. Assembly, configuration, and break-up history of Rodinia: a synthesis. Precambr. Res. 160, 179–210.
Loewy, S.L., Dalziel, I.W.D., Pisarevsky, S., Connelly, J.N., Tait, J., Hanson, R.E., Bullen, D., 2011. Coats Land crustal block, East Antarctica: a tectonic tracer for Laurentia? Geology 39, 859–862.
Lorenz, H., Gee, D.G., Larionov, A.N., Majka, J., 2012. The Grenville-Sveconorwegian orogen in the high Arctic. Geol. Mag. 149, 875–891.
Martin, E.L., Spencer, C.J., Collins, W.J., Thomas, R.J., Macey, P.H., Roberts, N.M.W., 2020. The core of Rodinia formed by the juxtaposition of opposed retreating and advancing accretionary orogens. Earth Sci. Rev., 103413
McLelland, J.M., Selleck, B.W., Bickford, M.E., Tollo, R.P., Bartholomew, M.J., Hibbard, J.P., Karabinos, P.M., 2010. Review of the Proterozoic evolution of the Grenville Province, its Adirondack outlier, and the Mesoproterozoic inliers of the Appalachians From Rodinia to Pangea: The Lithotectonic Record of the Appalachian Region. Geol. Soc. Am. Memoir 206, 21–49.
Merdith, A.S., Collins, A.S., Williams, S.E., Pisarevsky, S., Foden, J.D., Archibald, D.B., Blades, M.L., Alessio, B.L., Armistead, S., Plavsa, D., Clark, C., 2017. A full-plate global reconstruction of the Neoproterozoic. Gondwana Res. 50, 84–134.
Milnes, A., Wennberg, O., Skår, Ø., Koestler, A., 1997. Contraction, extension and timing in the South Norwegian Caledonides: the Sognefjord transect. In: Geological Society, London, Special Publication, pp. 123–148.
Möller, A., O'Brien, P.J., Kennedy, A., Kröner, A., 2002. Polyphase zircon in ultrahigh-temperature granulites (Rogaland, SW Norway): constraints for Pb diffusion in zircon. J. Metamorph. Geol. 20, 727–740.
Möller, C., Andersson, J., Dyck, B., Antal Lundin, I., 2015. Exhumation of an eclogite terrane as a hot migmatitic nappe, Sveconorwegian orogen. Lithos 226, 147–168.
Möller, C., Andersson, J., 2018. Metamorphic zoning and behaviour of an underthrusting continental plate. J. Metamorph. Geol. 36, 567–589.
Park, R.G., 1992. Plate kinematic history of Baltica during the Middle to Late Proterozoic: a model. Geology 20, 725–728.
Pedersen, S., Andersen, T., Konnerup-Madsen, J., Griffin, W.L., 2009. Recurrent Mesoproterozoic continental magmatism in south-central Norway. Int. J. Earth Sci. 98, 1151–1171.
Pesonen, L.J., Mertanen, S., Veikkolainen, T., 2012. Paleo-Mesoproterozoic supercontinents–a paleomagnetic view. Geophysica 48, 5–47.
Petersson, A., Scherstén, A., Bingen, B., Gerdes, A., Whitehouse, M.J., 2015. Mesoproterozoic continental growth: U-Pb–Hf–O zircon record in the Idefjorden terrane, Sveconorwegian Orogen. Precambr. Res. 261, 75–95.
Peron-Pinvidic, G., Osmundsen, P.T., 2020. From orogeny to rifting: insights from the Norwegian 'reactivation phase'. Sci. Rep. 10, 14860.
Pisarevsky, S.A., Elming, S.Å., Pesonen, L.J., Li, Z.X., 2014. Mesoproterozoic paleogeography: Supercontinent and beyond. Precambr. Res. 244, 207–225.
Poole, G.H., Kemp, A.I., Hagemann, S.G., Fiorentini, M.L., Jeon, H., Williams, I.S., Zappettini, E.O., Rubinstein, N.A., 2020. The petrogenesis of back-arc magmas, constrained by zircon O and Hf isotopes, in the Frontal Cordillera and Precordillera, Argentina. Contrib. Miner. Petrol. 175, 1–21.
Rey, P., Burg, J.-P., Casey, M., 1997. The Scandinavian Caledonides and their relationship to the Variscan belt. In: Geological Society, London, Special Publication, pp. 179–200.
Røhr, T.S., Corfu, F., Austrheim, H., Andersen, T.B., 2004. Sveconorwegian U-Pb zircon and monazite ages of granulite-facies rocks, Hisarøya, Gulen, Western Gneiss Region, Norway. Norwegian Journal of Geology 84, 251–256.
Røhr, T.S., Bingen, B., Robinson, P., Reddy, S.M., 2013. Geochronology of Paleoproterozoic augen gneisses in the Western Gneiss Region, Norway: evidence for Sveconorwegian zircon neocrystallization and Caledonian zircon deformation. J. Geol. 121, 105–128.
Roberts, N.M.W., 2010. From crystal to crust: the Proterozoic crustal evolution of southwest Norway. Doctoral dissertation. University of Leicester).
Roberts, N.M., Slagstad, T., Parrish, R.R., Norry, M.J., Marker, M., Horstwood, M.S., 2013. Sedimentary recycling in arc magmas: geochemical and U-Pb–Hf–O constraints on the Mesoproterozoic Suldal Arc, SW Norway. Contrib. Miner. Petrol. 165, 507–523.
Roberts, N.M., 2013. The boring billion?–Lid tectonics, continental growth and environmental change associated with the Columbia supercontinent. Geosci. Front. 4, 681–691.
Roberts, N.M., Slagstad, T., 2015. Continental growth and reworking on the edge of the Columbia and Rodinia supercontinents; 1.86–0.9 Ga accretionary orogeny in southwest Fennoscandia. Int. Geol. Rev. 57, 1582–1606.
Roffeis, C., Corfu, F., Gabrielsen, R.H., 2013. A Sveconorwegian terrane boundary in the Caledonian Hardanger-Ryfylke Nappe Complex: the lost link between Telemarkia and the Western Gneiss Region? Precambr. Res. 228, 20–35.
Roffeis, C., Corfu, F., 2014. Caledonian nappes of southern Norway and their correlation with Sveconorwegian basement domains. In: Geological Society, London, Special Publication, pp. 193–221.
Rudnick, R.L., Gao, S., 2003. Composition of the Continental Crust. Treatise on Geochemistry, 3. Elsevier, pp. 1–64.
Schärer, U., Wilmart, E., Duchesne, J.C., 1996. The short duration and anorogenic character of anorthosite magmatism: UPb dating of the Rogaland complex, Norway. Earth Planet. Sci. Lett. 13, 335–350.
Scheiber, T., Viola, G., Bingen, B., Peters, M., Solli, A., 2015. Multiple reactivation and strain localization along a Proterozoic orogen-scale deformation zone: the Kongsberg-Telemark boundary in southern Norway revisited. Precambr. Res. 265, 78–103.
Scherer, E., Münker, C., Mezger, K., 2001. Calibration of the lutetium-hafnium clock. Science 293, 683–687.
Sigmond, E.M.O., 1998. Geologisk kart over Norge, berggrunnskart Odda, 1:250000. Norges geologiske undersøkelse, Trondheim.
Skår, Ø., Pedersen, R.B., 2003. Relations between granitoid magmatism and migmatization: U-Pb geochronological evidence from the Western Gneiss Complex, Norway. Journal of the Geological Society 160, 935–946.
Slagstad, T., Roberts, N.M., Marker, M., Røhr, T.S., Schiellerup, H., 2013. A non-collisional, accretionary Sveconorwegian orogen. Terra Nova 25, 30–37.
Slagstad, T., Maystrenko, Y., Maupin, V., Gradmann, S., 2018a. An extinct, Late Mesoproterozoic, Sveconorwegian mantle wedge beneath SW Fennoscandia, reflected in seismic tomography and assessed by thermal modelling. Terra Nova 30, 72–77.
Slagstad, T., Roberts, N.M., Coint, N., Høy, I., Sauer, S., Kirkland, C.L., Marker, M., Røhr, T.S., Henderson, I.H., Stormoen, M.A., Skår, Ø., 2018b. Magma-driven, high-grade metamorphism in the Sveconorwegian Province, southwest Norway, during the terminal stages of Fennoscandian Shield evolution. Geosphere 14, 861–882.
Slagstad, T., Roberts, N.M., Kulakov, E., 2017. Linking orogenesis across a supercontinent; the Grenvillian and Sveconorwegian margins on Rodinia. Gondwana Res. 44, 109–115.
Slagstad, T., Marker, M., Roberts, N.M., Saalmann, K., Kirkland, C.L., Kulakov, E., Ganerød, M., Røhr, T.S., Møkkelgjerd, S.H., Granseth, A., Sørensen, B.E., 2020. The Sveconorwegian orogeny–reamalgamation of the fragmented southwestern margin of Fennoscandia. Precambr. Res. 105877.
Söderlund, U., Patchett, P.J., Vervoort, J.D., Isachsen, C.E., 2004. The 176Lu decay constant determined by Lu–Hf and U-Pb isotope systematics of Precambrian mafic intrusions. Earth and Planetary Science Letters 219, 311–324.
Söderlund, U., Hellström, F.A., Kamo, S.L., 2008. Geochronology of high-pressure mafic granulite dykes in SW Sweden; tracking the P-T-t path of metamorphism using Hf isotopes in zircon and baddeleyite. J. Metamorph. Geol. 26, 539–560.
Spencer, C.J., Roberts, N.M.W., Cawood, P.A., Hawkesworth, C.J., Prave, A.R., Antonini, A.S.M., Horstwood, M.S.A., 2014. Intermontane basins and bimodal volcanism at the onset of the Sveconorwegian Orogeny, southern Norway. Precambr. Res. 252, 107–118.
Spencer, C.J., Thomas, R.J., Roberts, N.M., Cawood, P.A., Millar, I., Tapster, S., 2015. Crustal growth during island arc accretion and transcurrent deformation, Natal Metamorphic Province, South Africa: new isotopic constraints. Precambrian Research 265, 203–217.
Spencer, C.J., Kirkland, C.L., Prave, A.R., Strachan, R.A., Pease, V., 2019. Crustal reworking and orogenic styles inferred from zircon Hf isotopes: proterozoic examples from the North Atlantic region. Geosci. Front. 10, 417–424.
Stephens, M.B., 2020. Chapter 8 - Outboard-migrating accretionary orogeny at 1.9–1.8 Ga (Svecokarelian) along a margin to the continent Fennoscandia. In: Geological Society, London, Memoirs, pp. 237–250.
Sundvoll, B., Larsen, B.T., 1994. Architecture and early evolution of the Oslo Rift. Tectonophysics 240, 173–189.
Swanson-Hysell, N.L., Kilian, T.M., Hanson, R.E., 2015. A new grand mean palaeomagnetic pole for the 1.11 Ga Umkondo large igneous province with implications for palaeogeography and the geomagnetic field. Geophys. J. Int. 203, 2237–2247.
Swanson-Hysell, N.L., Ramezani, J., Fairchild, L.M., Rose, I.R., 2019. Failed rifting and fast drifting: Midcontinent rift development, Laurentia's rapid motion and the driver of Grenvillian orogenesis. Bulletin 131, 913–940.
Tobi, A.C., Hermans, G.A., Maijer, C., Jansen, J.B.H., 1985. Metamorphic zoning in the high-grade Proterozoic of Rogaland-Vest Agder, SW Norway. In: Tobi, A.C., Touret, J.L. (Eds.), The deep Proterozoic crust in the north Atlantic provinces, NATO-ASI C158. Reidel, Dordrecht, pp. 477–497.
Tomkins, H.S., Williams, I.S., Ellis, D.J., 2005. In situ U-Pb dating of zircon formed from retrograde garnet breakdown during decompression in Rogaland, SW Norway. J. Metamorph. Geol. 23, 201–215.
Torsvik, T.H., Smethurst, M.A., Meert, J.G., Van der Voo, R., McKerrow, W.S., Brasier, M. D., Sturt, B.A., Walderhaug, H.J., 1996. Continental break-up and collision in the Neoproterozoic and Palaeozoic—a tale of Baltica and Laurentia. Earth Sci. Rev. 40, 229–258.
Torske, T., 1982. Structural effects on the Proterozoic Ullensvang Group (West Norway) relatable to forceful emplacement of expanding plutons. Geol. Rundsch. 71, 104–119.
Troch, J., Ellis, B.S., Harris, C., Bachmann, O., Bindeman, I.N., 2020. Low-$\delta^{18}O$ silicic magmas on Earth: a review. Earth Sci. Rev. 103299.
Tual, L., Pitra, P., Möller, C., 2017. P-T evolution of Precambrian eclogite in the Sveconorwegian orogen, SW Sweden. Journal of Metamorphic Geology 35, 493–515.
Tucker, R.D., Krogh, T.E., Raheim, A., 1990. Proterozoic evolution and age-province boundaries in the central part of the Western Gneiss Region, Norway: results of U-Pb dating of accessory minerals from Trondheimsfjord to Geiranger. In: Gower, C.F., Rivers, T., Ryan, A.B. (Eds.), Mid-Proterozoic Laurentia- Baltica. Geol. Assoc. Can. Spec. Pap. St. John's, Geological Association of Canada, pp. 149–173.
Ulmius, J., Andersson, J., Möller, C., 2015. Hallandian 1.45 Ga high-temperature metamorphism in Baltica: P-T evolution and SIMS U–Pb zircon ages of aluminous gneisses. SW Sweden. Precambrian Research 265, 10–39.
Vander Auwera, J., Bogaerts, M., Liégeois, J.P., Demaiffe, D., Wilmart, E., Bolle, O., Duchesne, J.C., 2003. Derivation of the 1.0–0.9 Ga ferro-potassic A-type granitoids of southern Norway by extreme differentiation from basic magmas. Precambrian Research 124, 107–148.
Vander Auwera, J., Bolle, O., Bingen, B., Liégeois, J.P., Bogaerts, M., Duchesne, J.C., De Waele, B., Longhi, J., 2011. Sveconorwegian massif-type anorthosites and related

granitoids result from post-collisional melting of a continental arc root. Earth Sci. Rev. 107, 375–397.
Vanderhaeghe, O., Teyssier, C., 2001. Partial melting and flow of orogens. Tectonophysics 342, 451–472.
Vanderhaeghe, O., 2012. The thermal–mechanical evolution of crustal orogenic belts at convergent plate boundaries: a reappraisal of the orogenic cycle. J. Geodyn. 56–57, 124–145.
Viola, G., Henderson, I.H.C., Bingen, B., Hendriks, B.W.H., 2011. The Grenvillian-Sveconorwegian orogeny in Fennoscandia: Back-thrusting and extensional shearing along the "Mylonite Zone". Precambr. Res. 189, 368–388.
Wain, A., 1997. New evidence for coesite in eclogite and gneisses: Defining an ultrahigh-pressure province in the Western Gneiss region of Norway. Geology 25, 927–930.
Waltenberg, K., Bodorkos, S., Armstrong, R., Fu, B., 2018. Mid-to lower-crustal architecture of the northern Lachlan and southern Thomson orogens: evidence from O-Hf isotopes. Aust. J. Earth Sci. 65, 1009–1034.
Wang, C.C., Jacobs, J., Elburg, M.A., Läufer, A., Elvevold, S., 2020. Late Neoproterozoic–Cambrian magmatism in Dronning Maud Land (East Antarctica): U–Pb zircon geochronology, isotope geochemistry and implications for Gondwana assembly. Precambrian Research 350, 105880.
Weber, B., Scherer, E.E., Schulze, C., Valencia, V.A., Montecinos, P., Mezger, K., Ruiz, J., 2010. U-Pb and Lu–Hf isotope systematics of lower crust from central-southern Mexico-Geodynamic significance of Oaxaquia in a Rodinia Realm. Precambr. Res. 182, 149–162.
Wennberg, O.P., Milnes, A.G., Winsvold, I., 1998. The northern Bergen Arc Shear Zone - an oblique-lateral ramp in the Devonian extensional detachment system of western Norway. Nor. Geol. Tidsskr. 78, 169–184.
Whitney, D.L., Evans, B.W., 2010. Abbreviations for names of rock-forming minerals. Am. Mineral. 95, 185–187.
Wiest, J.D., Jacobs, J., Ksienzyk, A.K., Fossen, H., 2018. Sveconorwegian vs. Caledonian orogenesis in the eastern Øygarden Complex, SW Norway – Geochronology, structural constraints and tectonic implications. Precambr. Res. 305, 1–18.
Wiest, J.D., Osmundsen, P.T., Jacobs, J., Fossen, H., 2019. Deep crustal flow within post-orogenic metamorphic core complexes – insights from the southern Western Gneiss Region of Norway. Tectonics 38, 4267–4289.
Wiest, J.D., Fossen, H., Jacobs, J., 2020a. Shear zone evolution during core complex exhumation – Implications for continental detachments. J. Struct. Geol. 140, 104139.
Wiest, J.D., Wrona, T., Bauck, M.S., Fossen, H., Gawthorpe, R.L., Osmundsen, P.T., Faleide, J.I., 2020b. From Caledonian Collapse to North Sea Rift: The Extended History of a Metamorphic Core Complex. Tectonics 39 e2020TC006178.
Wiest, J.D., Jacobs, J., Fossen, H., Ganerød, M., Osmundsen, P.T., 2021. Segmentation of the Caledonian orogenic infrastructure and exhumation of the Western Gneiss Region during transtensional collapse. J. Geol. Soc. https://doi.org/10.1144/jgs2020-199 jgs2020-2199.